INFLUENCE OF TEMPERATURE AND STRESS RATIO ON FATIGUE AND FRACTURE RESPONSE OF HPDC AM60B MAGNESIUM ALLOY

by

Md. Nur Hossain

Submitted in partial fulfilment of the requirements
for the degree of Master of Applied Science

at

Dalhousie University
Halifax, Nova Scotia
August 2010

DALHOUSIE UNIVERSITY

Department of Civil and Resource Engineering

The undersigned hereby certify that they have read and recommend to the Faculty of Graduate Studies for acceptance a thesis entitled "INFLUENCE OF TEMPERATURE AND STRESS RATIO ON FATIGUE AND FRACTURE RESPONSE OF HPDC AM60B MAGNESIUM ALLOY" by Md. Nur Hossain in partial fulfilment of the requirements for the degree of Master of Applied Science.

Dated: 19th August, 2010

Supervisor: _____

Readers: _____

_____

DALHOUSIE UNIVERSITY

DATE: 19th August, 2010

AUTHOR: Md. Nur Hossain

TITLE: INFLUENCE OF TEMPERATURE AND STRESS RATIO ON FATIGUE AND FRACTURE RESPONSE OF HPDC AM60B MAGNESIUM ALLOY

DEPARTMENT OR SCHOOL: Department of Civil and Resource Engineering

DEGREE: MASc CONVOCATION: October YEAR: 2010

Permission is herewith granted to Dalhousie University to circulate and to have copied for non-commercial purposes, at its discretion, the above title upon the request of individuals or institutions.

_____

Md. Nur Hossain

Dedicated to My Father

Md. Abdus Sattar

TABLE OF CONTENTS

LIST OF FIGURES

LIST OF TABLES

LIST OF ABBREVIATIONS AND SYMBOLS USED

a	Crack length
a_{avg}	Average crack length
ASTM	American Society for Testing and Materials
A	Amplitude ratio
b.c.c.	Body centred cubic
C_P	Paris model constant
CMVSS	Canadian Motor Vehicle Safety Standards
da/dN	Crack growth rate
E	Modulus of elasticity
E_f	Elongation
EDS	Energy dispersive X-ray analysis
F_X	Nodal force along the X direction
F_Y	Nodal force along the Y direction
FCGR	Fatigue crack growth rate
FEM	Finite element modelling
FCP	Fatigue crack propagation
FCPR	Fatigue crack propagation rate
G	The Strain energy release rate
HPDC	High pressure die cast

h.c.p.	Hexagonal close packed
K	Stress intensity factor
LBB	Leak before burst
LEFM	Linear elastic fracture mechanics
m_p	Paris model exponent
N_T	Total life
N_P	Propagation life
N_i	Initiation life
N.A.	Neutral axis
N	Number of cycles
P	Applied Load
PSBs	Persistent slip bands
P_{max}	Maximum load capacity
R	Stress ratio
SIF	Stress intensity factor
S-N	Stress-number of cycles
SENT	Single edge notched tension
SEM	Scanning electron microscope
T	Temperature
UTS	Ultimate tensile stress for in-grade lumber
u_{34}	Separation displacement between nodes 3 and 4 in X direction

v_{34}	Separation displacement between nodes 3 and 4 in Y direction
VCCT	Virtual crack closure technique
σ	Applied stress
σ_{max}	Maximum stress
σ_{min}	Minimum stress
σ_{mean} or σ_m	Mean stress
σ_{amp} or σ_a	Stress amplitude
σ_{true}	True stress
σ_{ult}	Ultimate tensile strength
$\sigma_{Engineering}$	Nominal Engineering stress
$\varepsilon_{Engineering}$	Nominal Engineering strain
ε_{true}	True strain
σ_{th}	Thermal stress
σ_y	Yield stress
α	Ratio of crack length to width of the specimen
α_1	Thermal expansion coefficient
ε	Total strain
ε_P	Plastic strain
ε_E	Elastic strain
γ	Material parameter used in Walker model
ΔT	Temperature difference
σ_t	Thermal stress
ΔK	Stress intensity factor range
ΔK_{eq}	Effective stress intensity factor range
Y	Geometric factor depending on the shape of the geometry
$\Delta\sigma$	Stress range

ACKNOWLEDGEMENTS

I am heartily thankful and would like to express honest gratefulness to my supervisor, Dr. Farid Taheri, whose encouragement, guidance and support from the initial to the final level enabled me to develop my research. I also wish to thanks the members of my thesis supervisory committee, Dr. Jane Thorburn and Dr. Kevin Plucknett for their advice and help. This research is carried out with the financial support provided by AUT021 Network of Centers of Excellence, an automotive research and development program focusing on issues relating to the automobile in the 21st century. I am really indebted to Auto 21 for their financial support.

Special and particular thanks are extended to Dr. Wood and Meridian Technologies Inc., (Strathroy, Ontario) for providing AM60B magnesium alloy for testing. I would like to appreciate with thanking to the Civil Engineering Department's technicians, Mr. Blair Nickerson and Brian Kennedy and my colleagues Kaveh, Nikzad, Julie, Mohammad, Mbarka, Shiva, Morteza, Pejman, Dr. Esmaeel and Dr. Taheri-Behrooz for their assistance with huge support and helping during my study and testing. It would not be justified if I don't mention the name of my friends Mushfiq, Murad, Tanim, Jhony and Iffat Jahan for their friendly support during my study.

Lastly, I offer my regards and blessings to my mother, Momtaz Begum and the rest of my family for their support and patience throughout the course of this study. I dedicate this thesis to the memory of my father, Md. Abdus Sattar whose unfailing support has always been the key to my success.

ABSTRACT

The mechanical behavior of a high pressure die cast AM60B Mg alloy is studied. Constant load amplitude fatigue tests were conducted at room, elevated and cold temperatures, with a stress ratio of R=0.1, and frequency of 30 Hz. The objective was to identify the possible effects of temperature on fatigue life cycle. In addition, fatigue crack propagation tests were conducted to ascertain the fatigue response of the alloy and determine its fatigue crack growth rate as a function of the applied stress ratio, experimentally, analytically and computationally, using Walker's model. The results demonstrated that temperature had a significant influence on the fatigue life, and that the life increased at cold temperature but decreased at elevated temperature as compared to that evaluated at room temperature. In this study, the limit for applicability of LEFM was established for AM60B magnesium alloy. In addition, fatigue crack propagation test results were used to evaluate the coefficients of the Paris model.

CHAPTER 1: INTRODUCTION

1.0 INTRODUCTION

Magnesium alloys are increasingly being utilized as one of the important structural materials due to their relatively light weight and high specific strength. Magnesium is the lightest structural metal available with a density of only 1.74 g/Cm^3, one quarter that of steel and two thirds that of aluminum (Lu, 2008). Among all other magnesium alloys, cast magnesium alloys are finding incremental usage in the automotive industry due to the above-mentioned attributes, as well as excellent castability and machinability. Currently, magnesium alloys are widely used for automobile components, mostly produced by high pressure die-casting process (Lu, 2008a). The general advantages of the die-casting process are: high productivity, high precision, good casting surface, fine solidification surface, and suitability for production of thin walled and complicated-shape components (Cahn et al., 1996). Therefore, the ongoing interest in the use of cast magnesium alloys in the automotive industry has recently triggered substantial research efforts to be focused on the characterization of the structural properties of the metals (Wang & Fan, 2006).

Moreover, applications of high pressure die-cast, HPDC AM60B magnesium alloy, such as front and support assemblies, steering wheel armature, instrument panel and steering column support brackets are playing a vital role in the automotive industry (Sun et al., 2007). The increased applications of the alloy in various fields require an in-depth understanding of the fatigue response and crack propagation behavior of the alloy under different load ratios. Moreover, it is well known that metal fatigue is significantly affected by changes in environment. Therefore, an important aspect in the life assessment of a metallic component is to investigate the material's fatigue performance at various temperatures.

On the other hand, it has been identified that the porosity level of materials can influence their mechanical properties, such as the ultimate tensile strength (UTS), 0.2% yield strength (YS), and the ultimate elongation (E_f) ((Gjestland et al., 2003), (Zhou, 2004)). Porosity is inherent in die-casting; it is mainly caused by turbulent flow of molten alloy during the high pressure filling of the mold (Lu, 2008). Fatigue resistance of the

magnesium alloys is affected by both gas and shrinkage pores. The α-Mg particles have a h.c.p. structure, whereas, the β-phase particles have a b.c.c. structure. Due to this difference and incompatibility of atomic structure, the (α–β) interface is either partially coherent or incoherent, which might be one of the significant reasons in facilitating a crack path and fatigue crack propagation.

1.1 MOTIVATION

As stated, the fatigue and fracture response of materials are influenced by several factors such as temperature and stress ratio in real life applications. Nevertheless, in the context of Mg alloys, investigations into the effects of the above factors are scarce. The motivation of this research is due to the increased applications of Mg alloy in the auto and aerospace industries. Therefore, characterization of the fatigue and fracture responses of HPDC AM60B Mg alloy at various temperatures and stress ratios is the main objective and motivator of this research. The aim is to gain a better understanding of the fatigue response of the alloy, thus further promoting the use of the alloy in the automotive industry. As such, a series of experimental, analytical and computational investigations were conducted in this project to characterize the fatigue and fracture response of HPDC AM60B magnesium alloy, which was provided by Meridian Technologies Inc. (Strathroy, Ontario).

1.2 OBJECTIVES

This thesis is based on the research that consisted of firstly a set of experimental, numerical and finite element analyses, and secondly, factographic studies with the aim of to characterizing the fatigue and fracture of HPDC AM60B magnesium alloy at room, elevated and low temperatures. From an implicational point of view, the research outcome would be very useful for not only the automotive and aerospace industries but also other applications where HPDC AM60B magnesium alloy might be of use in the future.

The influence of temperature on fatigue and fracture characterization of the HPDC AM60B magnesium alloy is one of the major concerns for its industrial applications. This research also aims to determine the most general trend of fatigue crack growth rate

(FCGR) variation as a function of the applied stress ratio, an extremely important factor for automotive and aerospace applications. As a result, different crack growth models are studied. The Walker model is successfully applied to consider the stress ratio impact on FCG of AM60B magnesium alloys. The overall objectives of this research can be summarized as:

1. To conduct an experimental investigation to characterize the fatigue response of HPDC AM60B magnesium alloy at room, elevated and low temperatures with a view to determining the influence of temperature on fatigue life cycle.
2. To evaluate the fatigue crack growth rate from fatigue crack propagation test results obtained experimentally and then to compare the results with those obtained through analytical and finite element methods.
3. To conduct factography studies on the failed specimens with the purpose of investigating the fracture nature of the alloy and further investigate the influence of temperature and stress ratio on fracture surfaces.

1.3 THESIS ORGANIZATION

This thesis is comprised of six chapters, which are organized as follows: the first chapter provides a short introduction to the topic, and states the motivation and objectives. A concise review of the pertinent literature is presented in chapter two. This review begins with a brief introduction, followed by outlining some of the pertinent concepts to assist the understanding of general fracture and fatigue phenomena. The three common approaches to fatigue design, characterized as stress, strain, and fracture mechanics-based, are also discussed. As well, common factors that affect the fatigue life of materials are briefly explained, as well as the factors that especially affect the cyclic response of magnesium alloys. chapters three to five present a series of technical papers that cover the various aspects of the experimental, analytical, and computational investigations carried out in this project. These papers have been accepted or submitted for publication in referred journals and conference proceedings. The content of chapter three has been submitted to Materials Characterization. The content of chapter four has been submitted to Journal of Materials Engineering and Performance. The content of chapter five has

been accepted for inclusion in the proceedings of COM 2010 (49th Annual Conference of Metallurgists) to be held in Vancouver, BC. October 3-6, 2010.

Finally, chapter six presents the conclusions of the research work and recommendations for future works.

CHAPTER 2: LITERATURE REVIEW

2.0 INTRODUCTION

This section offers a brief introduction, followed by definitions and an outline of the pertinent concepts related to fatigue and fracture phenomena in metals. Three common approaches for fatigue design, characterized as the stress, strain, and fracture mechanics-based approaches are also discussed. As well, the common factors that affect the fatigue life of magnesium alloys are briefly explained.

Very little research has thus far been done on fatigue and fracture characterization of magnesium alloys at elevated and low temperatures, and even less has been documented in relation to the specific grade of magnesium alloy studied in the present work (i.e. AM60B magnesium alloy). It is therefore timely and prudent to study the fatigue and fracture characterization of HPDC AM60B at elevated and low temperatures, as this magnesium alloy is increasingly being used in auto industry or in aerospace applications. For some applications as mentioned earlier, the above structural components might experience contact with elevated or low temperatures. For example, at high altitude, the frigid ambient air is known to enhance the fatigue life of HPDC AM60B magnesium alloy components (Suresh, 1998). According to the Canadian Motor Vehicle Safety Standards (CMVSS), climatic conditions as operation parameters and test conditions are categorized within two ranges of environmental temperature. Firstly, the range of -40ºC to 80ºC should be considered when parts are to be fitted in the passenger and luggage components, and secondly, the range of -40°C to 120°C should be considered for parts to be fitted in the engine components, unless otherwise specified.

2.1 BASIC DESIGN REQUIREMENT

A satisfactory level of performance and a well-established economy should be the top most priority for any structural design. Designers of machines, vehicles, and structures must achieve these acceptable levels of performance and economy. Vehicles and structures should be guaranteed to be safe and long-lasting. Excessive deformation, such as bending, twisting, or stretching of the structural components of a machine, vehicle, or any structure, should be avoided to assure safe performance and stability. In addition, it is necessary to avoid crack formation in components or limit crack formation and growth so

that it cannot progress into absolute fracture. The ancient structures that are still standing today obviously represent successful designs; however, there are undoubtedly many more unsuccessful designs that endured a much shorter life span (Anderson, 2000).

Mechanical behavior of materials is the study of their deformation and fracture in materials. Designing structures to avoid failure is not a new idea. This behavior of materials provides knowledge to avoid such kinds of failure in engineering applications. The important feature of this subject is that the samples of materials are physically tested by applying forces and deformations. Success in a particular engineering design can be evaluated from the behavior of a given material by testing it or from the published test data. The purpose of engineering design is to attain the geometry and dimensions of components such that they can perform their intended function in an economical, reliable and safe manner. Traditional and very general design approaches involve designing the components' cross-section such that the factored critical strength is greater than the factored applied stresses of the material. Structural failure must be avoided in design, so that the stress in a component would not exceed the strength of material.

During the design lifetime of any component, it is natural that a crack could occur either initially, due to material defects and the mechanized process, or over a certain period of time, due to decay in daily use. Brittle fracture can cause serious cracks and affect the strength and safety of the component, perhaps even causing it to break into two or more pieces at stress levels lower than that normally anticipated (Suresh, 1998), consequently, engineers should consider these concepts and ideas in design. It is necessary to avoid brittle rupture in design and to eliminate those structural details that might act as stress raisers and can be potential fracture-initiation sites. However, in most engineering structures, it is impractical and not impossible to eradicate all details and discontinuities.

2.2 MATERIAL FAILURE

The change in physical dimensions or shape of a component that causes the function of the components to be impaired is called deformation failure. Fracture is termed as the phenomenon of cracking due to the separation of the components into two or more pieces. Wear is the degradation of material due to chemical action and removal of surface covering due to abrasion coming into close contact between solid surfaces. When

abrasion is caused between fluid particles (gas or liquid) containing hard particles, it is termed as erosion.

The basic types of material failure that are classified as either deformation-based or fracture are indicated in Figure 2.1 (Dowling, 1998). Since several different causes exist, it is important to correctly identify the ones that may apply to a given design, so that the appropriate analysis methods can be selected to predict the behavior. With such a need for classification in mind, the various types of deformation and fracture are defined in this report.

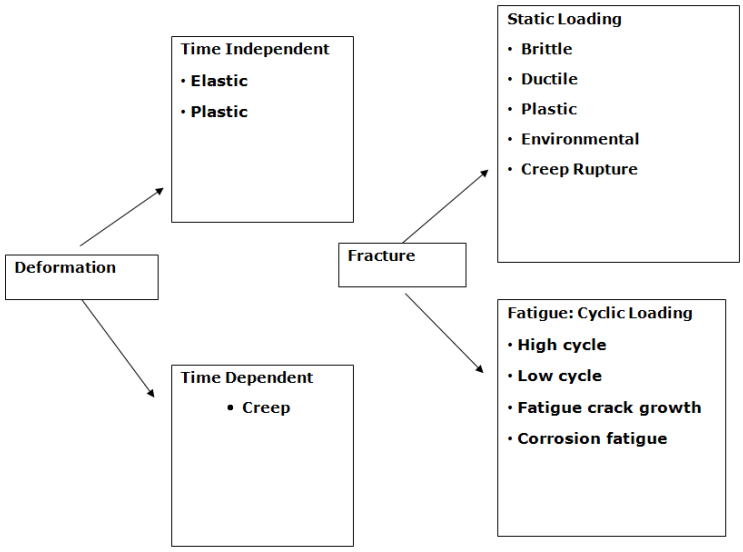

Figure 2.1 Basic types of deformation and fracture (Dowling, 1998)

2.3 DESIGN PHILOSOPHIES

Before designing a structure, it is important to ascertain the tolerable limit of the stresses of a given material for resistance calculations. For many applications, it is sufficient to determine the maximum static or dynamic stress that the material can withstand, and then design the structure to ensure that the stresses remain below acceptable limits. This involves fairly routine constitutive modeling and numerical or analytical solutions of appropriate boundary value problems. More critical applications require some kind of

defect tolerance analysis. In this regard, if a material or structure is considered to contain flaws, it will be decided whether to replace the part, or to leave it in service under a more acceptable loading for an assured period of time. Usually the discipline of Fracture Mechanics assists in making this kind of decision. As mentioned by Stephens et al., (2001), generally, four different design philosophies may be illustrated as follows:

"Infinite-Life Design: Unlimited safety is the oldest criterion. It requires local stresses or strains to be essentially elastic and safely below the pertinent fatigue limit. For parts subjected to millions of cycles, like engine valve springs, this is still a good design."
"Safe Life: The practice of designing for a finite life is known as "safe-life" design. It is used in many other industries too-for instance, in pressure vessel design and in jet engine design. The component is considered to be free of defects after fabrication and is designed to remain defect-free during service and withstand the maximum static or dynamic working stresses for a certain period of time."
"Fail Safe: When a component, structure, or vehicle reaches its allowable safe life, it must be retired before the average calculated life or test life is attained. This practice is very costly and wasteful. The component is designed to withstand the maximum static or dynamic working stresses for a certain period of time in such a way that its probable failure would not be catastrophic. For example, a pressure vessel designed to work under the leak-before-burst (LBB) condition should show leakage as a result of crack propagation. The aim is to prevent catastrophic failure by detecting the crack at its early stages of growth and also reducing the internal pressure."
"Damage Tolerance: This philosophy is a refinement of the fail-safe philosophy. It assumes that cracks will exist, caused either by processing or by fatigue, and uses fracture mechanics analyses and tests to determine whether such cracks will grow large enough to produce failures before they are detected by periodic inspections."

2.4 FUNDAMENTALS OF FATIGUE

Fatigue is commonly referred to as a process in which damage is accumulated in a material undergoing fluctuating loading, eventually resulting in failure, even if the maximum load is well below the elastic limit of the material. Fatigue refers to the process that reduces local strength of engineering materials (such as metallic alloys, polymers and

composites, including concrete and fiber reinforced plastics). ASTM has given the following definition of fatigue failures in all materials, though the phenomenological details of the process may differ from one material to another.

"Fatigue – the process of ***progressive localized*** *permanent structural change occurring in a material subjected to conditions that produce fluctuating stresses and strains at some point or points and that may culminate in cracks or complete fracture after a sufficient number of fluctuations."* (ASTM, 2000).

Fatigue is a continuous process in which damage initiates gradually in the primary stages and propagates very quickly towards the end. In most cases the initiation process is confined to a small area, usually of high local stress, where the damage accumulates during stressing. In adjacent parts of such components, where the stress level is low, no fatigue damage may occur and these parts thus would have an infinite fatigue life. The initiation process usually results in a number of micro-cracks that may grow more or less independently until one crack becomes dominant through a coalescence process as the micro cracks start to interact. Under steady fatigue loading, this crack grows slowly but starts to accelerate when the reduction of the cross-section increases the local stress field near the crack front. Final failure occurs as an unstable fracture when the remaining area is too small to support the load. These stages in the fatigue process can, in many cases, be related to distinctive features of the fracture surface of components that have failed under fluctuating loads; the presence of these features can therefore be used to identify fatigue as the probable cause of failure.

2.5: APPROACHES TO FATIGUE DESIGN

Post-fatigue life calculations could be considered to fall into three broad categories, as delineated below.

2.5.1 Stress-based Approach

Stress-based (S-N) methods are commonly used for components that are desired to have long lives. In comparison with strain-based approaches, stress-life (S-N) methods are easier to understand and require fewer calculations.

The stress-based approach covers the effects of stress concentrations, mean stresses, surface modifications, variable amplitude cyclic loads, and multiaxial loads (Suresh, 1998). The S-N method requires fatigue data in the form of curves of stress (S) vs. cycles to failure (N). Normally, smooth specimens are used to produce these curves. A finite element (FE) model could be used to give the peak stresses in a component and a life obtained by comparing this with S-N data from a series of smooth specimen tests.

2.5.2 Strain-based Approach

Strain-based fatigue methods are used especially for lives below about 10^4 or 10^5 cycles. Above these levels, stresses can exceed the elastic limit. Using stresses to assess damage at critical regions will hence be non-conservative, since they would no longer accurately represent the deformation a region undergoes if the yield limit of the material is exceeded. Strains are thus the more appropriate measure of the sustained fatigue damage. In many practical applications, engineering components generally undergo a certain degree of structural constraint and localized plastic flow, particularly at locations of stress concentrations. In these situations, it is more appropriate to consider the strain-life approach (Suresh, 1998).

2.5.3 Fracture Mechanics Approach

A third approach of fatigue design is fracture mechanics. The fracture mechanics approach considers the growth of an assumed crack to characterize fatigue and fracture, which differentiates it from the above two approaches. Determination of fracture parameters under various loading conditions is very important and crucial in any fatigue and fracture study. In the fracture mechanics approach, it is very common to characterize the fatigue and fracture phenomena with only one single parameter, such as the stress intensity factor, energy release rate, or J-integral. Any one of the above parameters could be the measure of fatigue and fracture characterization, depending on the applications.

2.6 FATIGUE TERMINOLOGIES

This section provides a brief introduction to the relevant terminologies used in fatigue design and analysis.

Stress range ($\Delta\sigma$): The stress range is defined as the difference between the maximum stress (σ_{max}) and the minimum stress (σ_{min}):

$$\Delta\sigma = \sigma_{max} - \sigma_{\min} \tag{2.1}$$

Mean stress: The mean stress is the average values of the maximum and minimum stresses, that is:

$$\sigma_{mean} = \frac{\sigma_{max}+\sigma_{\min}}{2} \tag{2.2}$$

Stress amplitude: The stress amplitude is half of the stress range, that is:

$$\sigma_{amplitude} = \frac{\sigma_{max}-\sigma_{\min}}{2} \tag{2.3}$$

Stress ratio: The stress ratio corresponds to the ratio between minimum stress and maximum stress and expresses the relative load in each cycle:

$$R = \frac{\sigma_{min}}{\sigma_{max}} \tag{2.4}$$

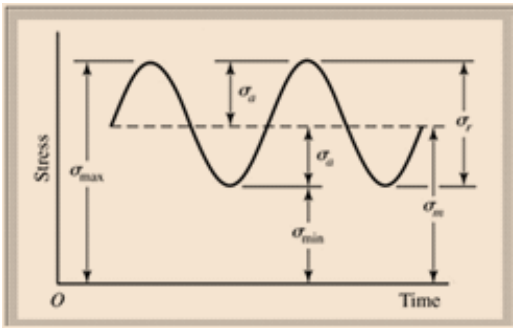

Figure 2.2 Constant amplitude cycling and the associated nomenclature (Dowling, 1998).

Fluctuating stresses in machinery often take the form of a sinusoidal pattern because of the nature of some of the rotating machinery. As well, other patterns, some quite irregular, do occur. Different loading scenarios are described in the Figures 2.3 to 2.5.

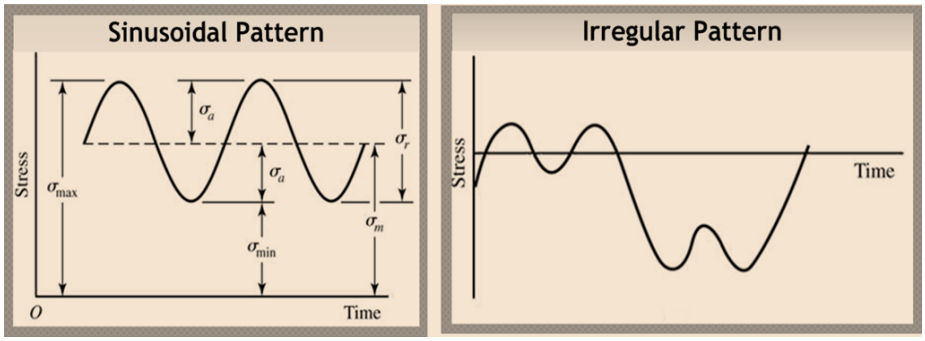

Figure 2.3 Illustration of the sinusoidal and irregular load patterns (Dowling, 1998)

From the Figures 2.3 to 2.5, it is possible to illustrate different loading cycles. Mainly, there exist three cases which are the most common and general from an implicational point of view. They are:

R=-1: This indicates a complete reversed loading corresponding to a minimum compressive stress to an equal maximum tensile stress.

R=0: This represents repeated one directional fluctuating loading with an applied minimum stress of zero, such that $\sigma_{mean} = 0.5\sigma_{max}$

And, $0 \leq R \leq 1$, representing not completely reversed loading, where, $\sigma_{mean} \neq 0$.

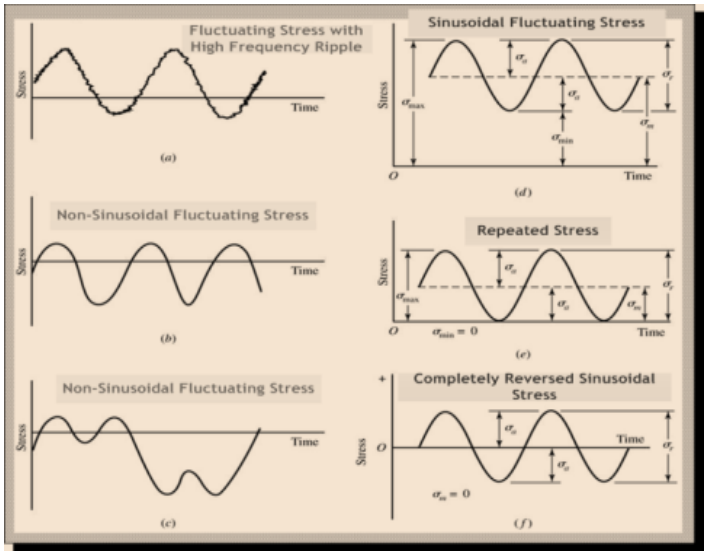

Figure 2.4 Illustration of various load patterns (Dieter, 1988)

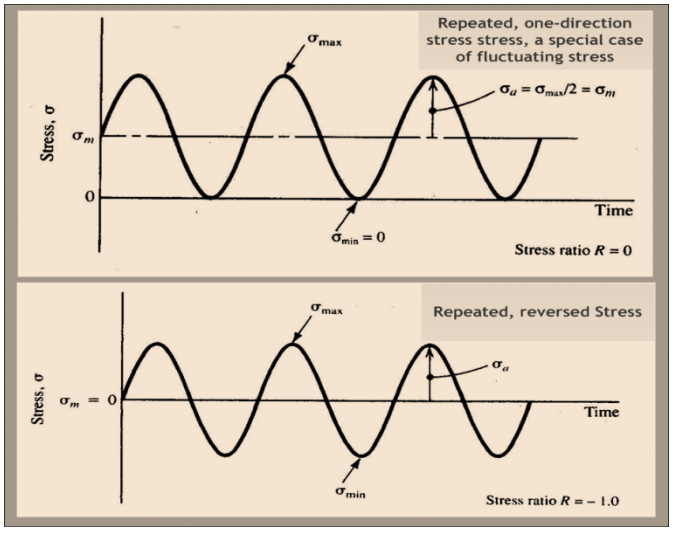

Figure 2.5 Illustration of the various load patterns (Dowling, 1998)

2.7 NATURE OF THE FATIGUE AND FRACTURE PROCESS

According to the description of the characteristics of fatigue and fracture surfaces, the fatigue process can be identified by the following stages:

- Stage I: Crack initiation
- Stage II: Propagation of one dominant crack
- Stage III: Final fracture

It is well known that fatigue cracking in metals is always allied with the accumulation of irreversible plastic strain. The following section provides a short discussion on fatigue and fracture phenomena related to different magnesium alloys based on a few articles available in public domain. Some of these alloys are related to the current study of fatigue and fracture characterization of AM60B magnesium alloys.

As stated earlier, in the application of high cycle fatigue, fatigue failure might occur even below the elastic limit of the material due to cyclic stress. In such a case, large-scale plastic deformation does not occur. However, this is not applicable on a free surface, where the plastic strains may accumulate as a result of dislocation movements. Dislocations are line defects which arise during crystal growth or as a result of mechanical deformation of a crystal. In any material structure, dislocations occurred within the lattice structure which can move and accelerate due to applied stress, leaving a permanent deformation. As there is no constraint from grain boundaries on free surfaces, deformation (or slip) is greater than that in the interior of crystalline materials.

In polycrystalline structural metals, grains are separately distributed in a random fashion. In such a distribution, each grain has an ordered atomic structure ensuring a rise to directional properties. Thus, the deformation takes place on crystallographic planes of easy slip, along which it is easier to move dislocations than on other planes, resulting in a roughening of the surface by slip bands. This slip band deformation is intensified at the surface and extends into the interior of the grain, resulting in the very common persistent slip bands (PSBs). Extrusions and intrusions are the accumulation of local plastic flow resulting in surface ridge and trough, respectively, as seen in Figure 2.6. Due to oxidation

of free surfaces, the cohesion between the layers in the slip band is weakened. During the process, small cracks develop in the intrusions, while in the shear stress driven process, micro cracks grow along slip planes.

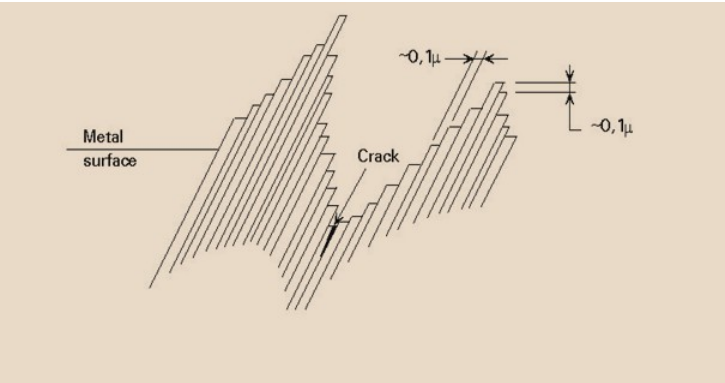

Figure 2.6 Slip band with extrusions and intrusions formed on the surface of grain subjected to cyclic stress (Suresh, 1998).

This growth tends to initiate in the shear mode, which extends over a few grains (this is identified as the stage I crack growth.) During continued applied cyclic loading, micro cracks in different grains begin to coalescence, resulting in either one or a few dominating cracks. Under the primary action of the maximum principal stress, the stress field associated with the dominating crack starts to propagate; this is called stage II growth, as shown in Figure 2.7.

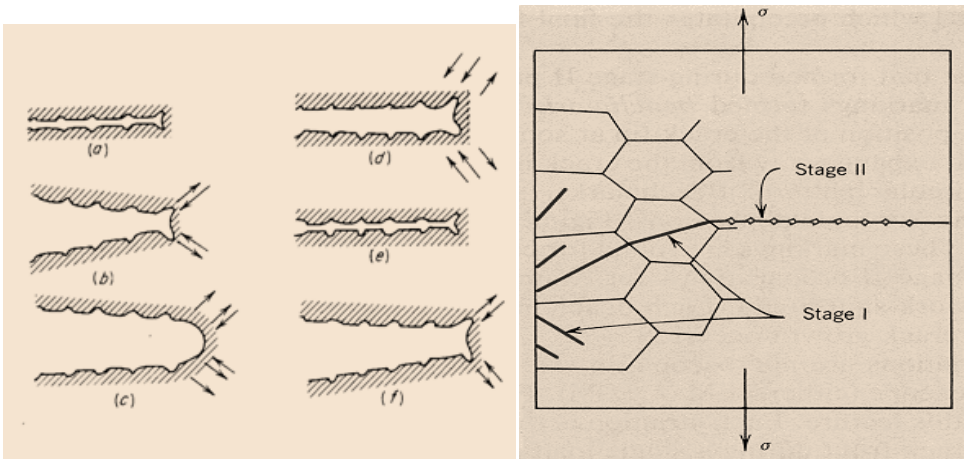

Figure 2.7 Plastic blunting processes for growth of stage II fatigue crack (Laird, 1967).

While the crack path would be essentially perpendicular to the axis of the tensile stress, the resulting crack propagation would, however, be still biased by the crystallographic orientation of the grains. Thus, the crack proceeds in an irregular and zigzag path along the slip and cleavage planes from grain to grain, resulting in final fracture (stage III). Within this stage, the progressive fatigue cracks initiate, for example, micro-cracks can be initiated from the striations, leading to a cleavage fracture.

In view of the fact that crack nucleation is related to the level of stress, any stress concentration in the form of external or internal surface flaws can manifest reduced fatigue life, especially when the initiation phase occupies a considerable portion of the total life. Thus, it is obvious that a part with a smooth, polished surface would normally have a higher fatigue strength than the one with a rough surface. It is also possible to initiate a crack facilitated by inclusions, which act as internal stress raisers. Slip band deformations at inclusions are higher in ductile materials than elsewhere and fatigue cracks may nucleate here if there are no other raisers to dominate.

Sometimes, different initiation mechanisms are observed in high-strength materials. The interface between the matrix and inclusion may be comparatively weak, and as a result, cracks may initiate in such regions if decohesion occurs at the inclusion surface followed by the increased stress/strain field around the inclusion. Alternatively, a hard brittle inclusion may rupture and a fatigue crack may initiate at the edges of the cleavage fracture.

Ishihara et al. (2009) considered the fatigue crack growth behavior of AZ31, an extruded magnesium alloy. According to the authors, fatigue cracks were initiated at an early stage (i.e., 5-10% of fatigue life), which clearly indicated that the majority of fatigue life was engaged in crack propagation.

From the discussion above, it is evidently not possible to make a clear distinction between crack nucleation and stage I growth. "Crack initiation" is thus a rather imprecise term used to describe a series of events leading to a stage II crack. Although the initiation stage includes some crack growth, the small scale of the crack compared with micro-structural dimensions such as grain size invalidates a fracture-mechanics-based analysis

of this growth phase. Instead, local stresses and strains are commonly related to material constants in prediction models used to estimate the length of stage I. The material constants are normally obtained from tests on smooth specimens subjected to stress- or strain-controlled cycling.

2.8 FATIGUE FRACTURE CHARACTERISTICS OF DIE-CAST MAGNESIUM ALLOY

Figure 2.8 shows the microstructure of HPDC AM60B magnesium alloy, which is very typical of most of the magnesium-aluminum-manganese alloys in which there are grains of an Mg-rich solid solution called α-Mg with the hexagonal close packed, h.c.p. structure and secondary β-$Al_{12}Mg_{17}$ phase of a body centered cubic, b.c.c. structure. In addition to the above primary and secondary phases, there is an intermetallic phase of the AlMnSi. The presence of brittle β-$Al_{12}Mg_{17}$ particles has a significant influence on the mechanical properties of cast magnesium alloys.

Shih et al. (2002) investigated the fatigue properties of extruded AZ61A magnesium alloys. Their fractography study indicated that fatigue cracking initiated from subsurface or surface inclusions. Near the surface, these inclusions served as stress raisers and induced clusters of slip bands. After initiation, the cracks grew under the dominant shear stress and resulted in a cleavage fracture, as shown in Figure 2.9.

Wang et al. (2006) studied the low-cycle fatigue small crack initiation and propagation behavior of cast magnesium alloys (AM50 and AM60) based on in–situ SEM observations. The results indicate that the small fatigue crack formed preferentially on β-$Al_{12}Mg_{17}$ boundaries at room temperature and initially propagated along the interface of α-Mg grains due to a micro-mechanism of the accumulative plastic slipping of surface grains (α-Mg).

Zenga et al. (2009) investigated the fatigue crack propagation behavior of an extruded magnesium alloy AZ80. On the basis of their results, it was demonstrated that the fatigue crack propagation behavior for the extruded magnesium alloy is concerned with the coalescence of micro-voids.

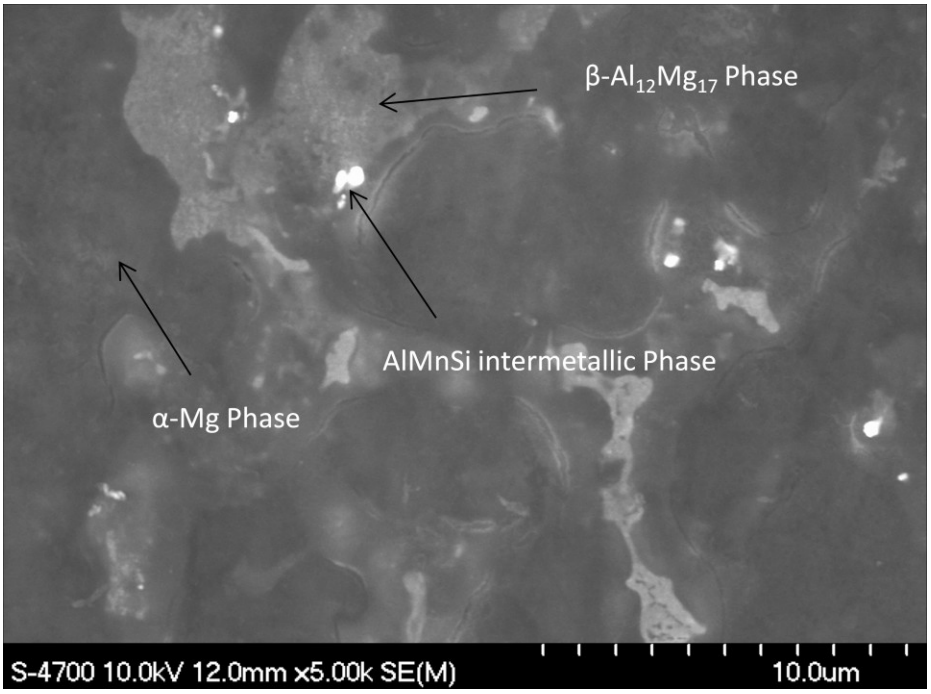

Figure 2.8 Microstructure of AM60B magnesium alloy.

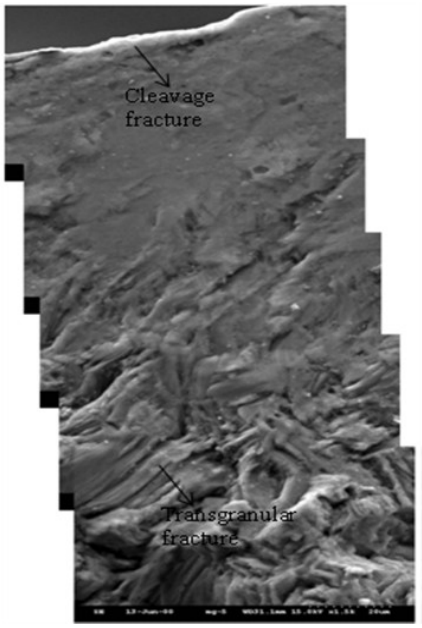

Figure 2.9 SEM micrograph displaying the fracture of a specimen subjected to stress amplitude of 200 MPa, failed at 1.48×104 cycles, including cleavage fracture near the surface and trans-granular fracture (Shih et al. 2002).

2.9 PRIMARY FACTORS AFFECTING FATIGUE LIFE

2.9.1 Modifying Factors

The difference in fatigue behavior of full scale machine or structural components, as compared with small laboratory specimens of the same material, is sometimes striking. In the majority of cases, the real life component exhibits a considerably poorer fatigue performance than the laboratory specimen although the computed stresses are the same. This difference in fatigue response can be examined in a systematic manner by evaluating the various factors that influence fatigue strength. Qualitative and quantitative assessments of these effects are presented in the following paragraphs. There are some modifying factors that affect fatigue life called primary factors. They are:

i. Sample size
ii. Type of loading
iii. Surface finish
iv. Surface treatments
v. Test temperature
vi. Environment

The presence of a notch in components decreases their fatigue life through creation of stress concentration. Surface roughness also lowers life, again through stress concentration. Moderate compressive stress at the surface increases life (shot peening), as it is harder to nucleate a crack when the local stress state opposes crack opening. In addition, a corrosive environment lowers the life, as corrosion either increases the rate at which material is removed from the crack tip and/or it produces material on the crack surfaces that force the crack open (e.g. oxidation).

Anything on the surface that is a site of stress concentration would promote crack formation and consequently shorten the time required for nucleation of cracks. Defects in the material or the existence of a void or a hard particle inside the material can reduce the stress and/or strain required to nucleate a crack, again shortening the time required for nucleation of cracks. Regarding dislocation slip characteristics, if dislocation glides are confined to particular slip planes (called the planar slip), then the dislocations can pile up

at any grain boundary, or phase boundary. A stress concentration could be developed on the head of the pile-up, consequently initiating a crack depending on the adjacent grain orientation.

The main effect of microstructure (defects, surface treatment, etc.) is almost all in the low stress intensity regime (i.e. stage I). Defects, for example, make it easier to nucleate a crack, which translates into a lower crack propagation threshold (ΔK_{th}).

Voids are introduced in cast metals either by gas evolution during their solidification or by shrinkage or by incomplete sintering in powder consolidation. Inclusions are entrained during the phase of solidification in a material. In metals, inclusions are generally oxides migrating from the surface of the metal melt or a slag.

Corrosion in fresh or salt water can have a very detrimental effect on the fatigue strength of engineering materials. Even distilled water may reduce the high-cycle fatigue strength to less than two-thirds of its value in dry air. Protection against corrosion can successfully be achieved by surface coatings, either by paint systems or through the use of metal coatings. Coated metal is deposited either by galvanic or electrolytic deposition or by spraying. The preferred method of corrosion protection for marine structures, however, is cathodic protection, which is obtained by the use of sacrificial anodes or, more infrequently, by impressed current.

Environment has a huge impact on fatigue life of magnesium alloy. Heuler et al. (2008) investigated the environmental impact on fatigue life of magnesium alloys. It was found that the degradation of fatigue behavior in chloride-containing media is not simply determined by the external corrosive attack but also influenced by inner defects competing with the environmental impact.

Eliezer et al. (2001) studied the corrosion fatigue of die-cast and extruded magnesium alloys. A corrosive environment (3.5 % NaCl) significantly decreases fatigue life of alloys, especially for extruded alloys. Extruded alloys show higher sensitivity to the action of NaCl solution in comparison with die-cast alloys.

As stated earlier, the presence of a notch would have a tremendous impact on short crack propagation. Verreman and Limodin et al. (2008) studied the notch effect on fatigue crack propagation. Fatigue life of notched components cannot be predicted using data only from smooth specimens. It was observed that the more severe the notch, the shorter was the crack initiation life, and the larger the short crack propagation life.

Residual stresses have a similar influence on fatigue life as externally imposed mean stresses (i.e., a tensile stress reduces fatigue life while a compressive stress increases life). There is, however, an important difference which relates to the stability of residual stresses. While an externally imposed mean stress (e.g. stress caused by the components self-weight) would always act, thus, residual stress may relax with time, especially if there are high peaks in the load spectrum that cause local yielding at stress concentrations.

In magnesium alloys, there is a hierarchy of names for second phase particles: *inclusions* are unwanted oxides (e.g. MgO), *dispersions* are intermetallic particles that, once precipitated, are thermodynamically stable (e.g. MgAlSi compounds), while *precipitates* are intermetallic particles that can be dissolved or precipitated depending on temperature.

2.9.2 Mean Stress and Temperature Effect on Fatigue Life of Die-Cast Magnesium Alloy

2.9.2.1 Mean Stress Effect

As stated, since the main objective of this research to investigate the influence of stress ratio and temperature on the fatigue response of AM60 Mg alloy, a brief discussion on the effect of the parameters is offered in the following section.

In 1870, Wohler identified stress amplitude as the primary loading variable in fatigue testing; however, the static or mean stress also affects fatigue life. In general, a tensile mean stress reduces fatigue life while a compressive mean stress increases life. Mean stress effects are presented either by the mean stress itself, as a parameter, or the stress ratio, R. The two are interrelated through:

$$\sigma_m = \sigma_a^{\frac{1+R}{1-R}} \quad (2.5)$$

Ishihara et al. (2009) explained that the influence of mean stress on the fatigue strength can be described approximately by the Gerber relationship. This is as follow.

$$\sigma = \sigma_{(R=-1)}\{1 - (\frac{\sigma_m}{\sigma_{ult}})^2\} \quad (2\text{-}6)$$

Zenga et al. (2009) investigated fatigue crack propagation (FCP) behavior of an extruded magnesium alloy AZ80. On the basis of the results, it was demonstrated that loading ratio had a significant influence on fatigue crack propagation rate and that it increased with an increase in stress ratio, as shown in Figure 2.10. It was demonstrated that more pronounced fracture was found in the SEM images for the case of specimens tested at higher stress ratios. Some fracture surfaces at different stress intensity factor ranges and frequencies are shown in Figure 2.11.

2.9.2.2 Temperature Effect

During heating or cooling, a thermal stress is developed which is responsible for thermal fatigue. Thermal fatigue is created at high temperature by fluctuating *thermal stresses* (σ_{th}).

The basic formula of the temperature effect is:

$$\sigma_{th} = E\,\alpha_l\,\Delta T \quad (2\text{-}7)$$

where, α_l is the linear thermal expansion coefficient, E is the modulus of elasticity and ΔT is the temperature difference.

For some materials, it is a common tendency to increase the fatigue strength and endurance limit as temperature is decreased. On the other hand, fatigue strength is decreased due to increase in temperature. This is why fatigue is very dependent on temperature.

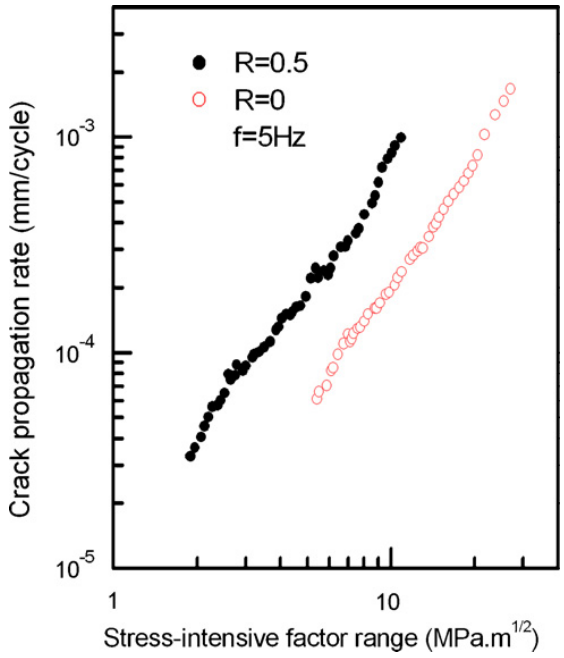

Figure 2.10 Influence of load ratio on the fatigue crack propagation (FCP) rate of as-extruded magnesium alloy AZ80 (Zenga et al., 2009).

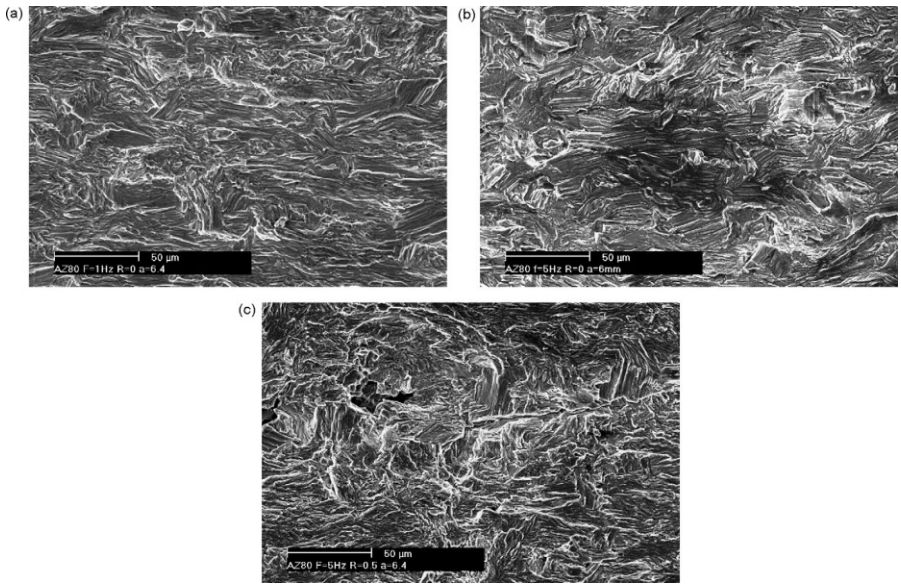

Figure 2.11 SEM micrograph showing fracture surface at (a) $\Delta K = 5.3$ MPa$\sqrt{\mathbf{m}}$ at R = 0 and f = 1 Hz, (b) $\Delta K = 5.1$ MPa$\sqrt{\mathbf{m}}$ at R = 0 and f = 5 Hz and (c) $\Delta K = 5.8$ MPa$\sqrt{\mathbf{m}}$ at R = 0 and f = 5 Hz (Zenga et al., 2009).

Grinberg et al. (1979) described the effect of low temperature on the fatigue failure of a MA12 magnesium alloy. According to the author's results, it was identified that reductions in temperature lead to an increase in fatigue limit. When the temperature was reduced from 20° to -120°C, with identical cyclic loading, the fatigue life of MA12 magnesium alloy was increased.

Sajuri et al. (2005) studied the effects of humidity and temperature on the fatigue behavior of an extruded AZ61 magnesium alloy. According to their results, it was found that a significant reduction in fatigue strength was observed with an increase of temperature to 150°C. SEM fractographs of fracture surfaces were also investigated (see Figures 2.12 and 2.13).

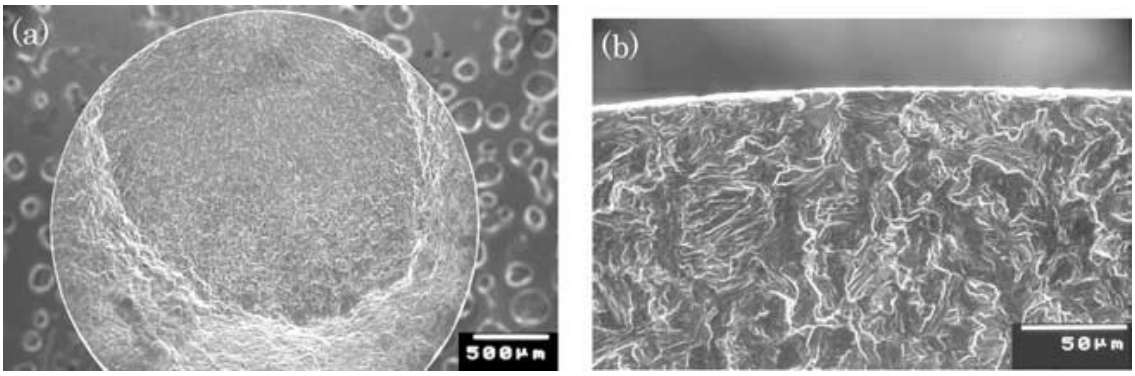

Figure 2.12 SEM fractographs showing (a) overview of the fracture surface and (b) transgranular crack initiation and propagation in a specimen tested at 180 MPa at 20°C with 80% relative humidity (Sajuri et al. 2005).

Xi-shu and Jing-hong et al. (2006) studied the fatigue growth rate in cast AM50 magnesium alloy. They found that the growth rate of small fatigue cracks increased when temperature increased.

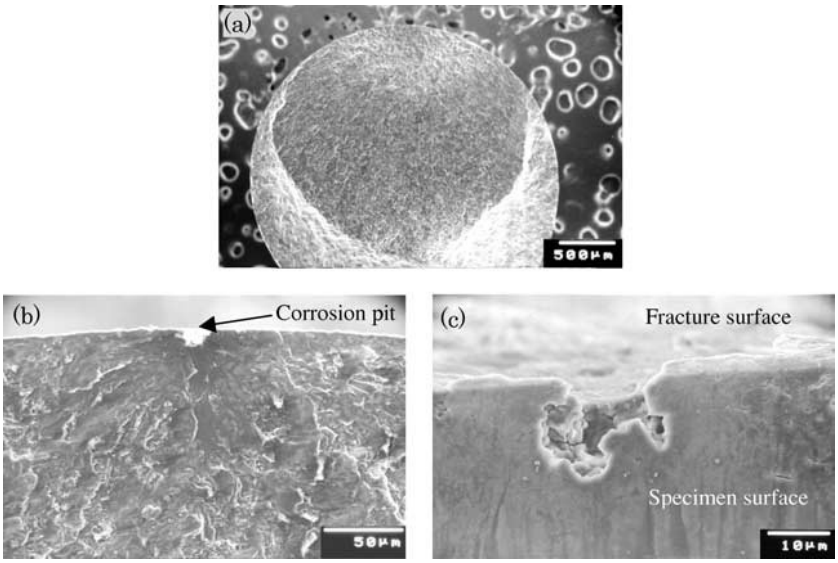

Figure 2.13 SEM fractographs showing (a) overview of the fracture surface (b) formation of corrosion pit, fatigue-crack initiation and propagation and (c) specimen surface corrosion pit in specimen tested at 130 MPa at 50ºC with 80% relative humidity (Sajuri et al. 2005).

Many materials undergo a significant reduction in fracture toughness at low temperature, which makes temperature one of the most important design considerations. There would be a reasonable variation and change in the fatigue properties of a material under the influence of temperature. The resulting change would appear sometimes in the form of an intergranular fracture, from grain to grain boundary, and sometimes as a transgranular crack with a ductile, brittle or cleavage fracture.

Wang and Jan et al. (2006) studied the fatigue growth rate in cast AM50 magnesium alloy. They noted that small fatigue cracks propagated preferentially through dendrite cells and along interdendritic regions at elevated temperatures. However, cracks propagated mainly through interdendric regions at room temperature. This is because those regions have been weakened by intensive dislocations activity.

Venkateswarana et al. (2004) observed that AZ91D magnesium alloy failed in a brittle manner at room temperature and that the fracture surfaces showed the quasi-cleavage mode of fracture, as investigated by SEM (see Figures 2.14 and 2.15).

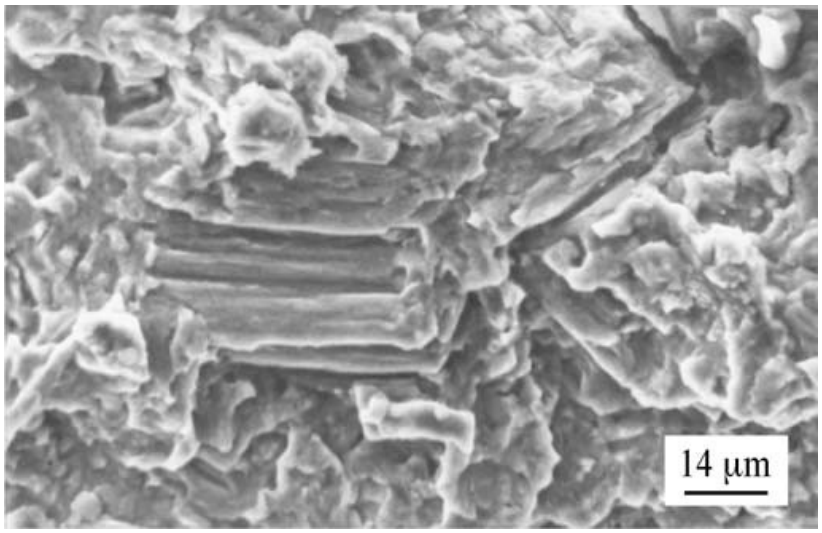

Figure 2.14 Fractograph of fatigue-tested AZ91D alloy at a maximum stress of 40 MPa showing quasi-cleavage fracture (Venkateswarana et al. 2004).

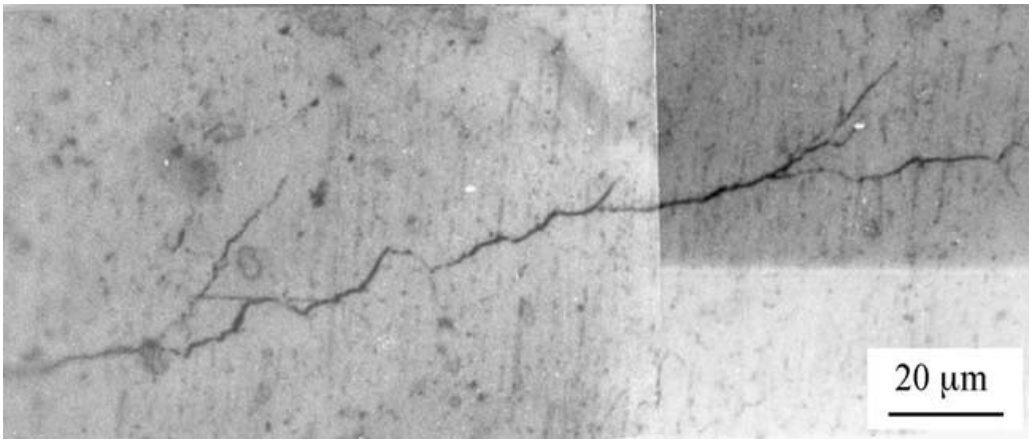

Figure 2.15 Branching and deflection of a crack in a specimen tested at a maximum stress of 35 MPa (Venkateswarana et al. 2004).

CHAPTER 3: INFLUENCE OF ELEVATED TEMPERATURE AND STRESS RATIO ON THE FATIGUE RESPONSE OF AM60B MAGNESIUM ALLOY

Md. Nur Hossain and Dr. Farid Taheri

Publication Status: Submitted to Materials Characterization (an International Journal on Materials Structure and Behavior)

3.0 ABSTRACT

The mechanical behavior of a high pressure die-cast AM60B Mg alloy was studied at elevated temperature. The fatigue tests were conducted with stress ratio of R=0.1, and frequency of 30 Hz. The objective was to identify the possible effect of temperature on the alloy's fatigue life cycle. In addition, fatigue crack propagation tests were conducted to ascertain the fatigue response of the alloy and determine the fatigue crack growth rate, in consideration of the influence of stress ratio on the basis of the Walker model.

Keywords AM60B magnesium alloy, LEFM (Linear Elastic Fracture Mechanics), SENT (Single Edge Notch Tension), FCGR (Fatigue Crack Growth Rate), FEM (Finite Element Method). SEM (Scanning Electron Microscope)

3.1 INTRODUCTION

Magnesium alloys are increasingly being used in the automobile and light truck industries. Among all other magnesium alloys, cast magnesium alloys are finding incremental use in the automotive industry due to their high specific strength, lower density and excellent castability and machinability in comparison to the commonly used metallic materials. As a result, ongoing interest in the use of cast magnesium alloys in the automotive industry has recently triggered substantial research efforts to be focused on characterization of the structural properties of the metals (Wang & Fan, 2006). The increased use of the alloy in various fields demands knowledge about the fatigue properties and fracture response of the alloy. Therefore, before utilization of magnesium alloys in most mechanical and structural applications, the determination of their fatigue lives and crack propagation characteristics at different stress ratios is necessary. Moreover, depending on the application, the environment might play a vital role on the fatigue life cycle of these alloys, since it is well established that metals fatigue life cycles are markedly affected by changes in their environment (Grinberg et al. 1977).

Assessment of fatigue performance, at room or elevated temperatures, is an integral part of the life assessment of any component, especially those employed in automobiles. As the uses of cast magnesium alloys is gaining higher demand in structural and high temperature applications, the understanding of fatigue response of such cast alloys at elevated temperature becomes more imperative.

In this study, one of the well-known structural magnesium alloys, AM60B, which has been characterized as an alloy with outstanding ductility and energy absorbing properties, combined with good strength, light weight and castability, is considered. Materials, especially those with relatively low fracture toughness, might fail even below their ultimate strength. The failure can be analyzed on the basis of linear elasticity concepts, through the use of the linear elastic fracture mechanics (LEFM) [(Stephens et al. 1980)]. High strength, light weight metallic alloys, such as those used in aerospace industry, are examples of such materials (Stephens et al. 1980). By using LEFM, it is possible to make a direct comparison of fatigue crack growth behavior of the engineering components or

structures and their counterpart laboratory specimens, using the stress intensity factor range, ΔK (Dowling, ,1998).

There has been some work done in recent years on characterizing the fatigue response of various die-cast magnesium alloys. However, the work on high pressure die cast, HPDC magnesium alloys has been quite limited. Koch (2004) investigated the fatigue limit of HPDC AM60 magnesium alloy. Later, Lu (2008) reported the fatigue characterization of HPDC AM60B magnesium alloy at room temperature. However, the above authors did not investigate the fatigue response of the alloy at elevated temperature.

One of the few works investigating the influence of temperature on the fatigue of such alloys has been the work of Wang et al. (2006); they investigated the fatigue crack growth behavior of AM50 magnesium alloy at elevated temperature. They found that the growth rate of small fatigue cracks increased when temperature increased. Moreover, investigation into the influence of stress ratio on the fatigue response of these alloys is as scarce. One of the few notable works on this topic is that by Ishihara et al. (2009), who explained that the influence of mean stress on the fatigue strength can be described approximately by the Gerber relationship. This is as follow.

$$\sigma = \sigma_{(R=-1)}\{1 - (\frac{\sigma_m}{\sigma_{ult}})^2\} \qquad (3\text{-}1)$$

where σ is the stress amplitude corresponding to the fatigue strength at a given mean stress σ_m; $\sigma_{(R=-1)}$ is the fatigue strength at R=-1, and σ_{UTS} is the ultimate tensile strength.

Zenga et al. (2009) also observed that the loading ratio had a significant influence on the fatigue crack propagation rate of an extruded magnesium AZ80 alloy, and that it increased with an increase in load ratio.

The lack of information on the influence of temperature and stress ratio on the fracture and fatigue of response of HPDC AM60 magnesium alloy therefore motivated the work presented here. In the present study, static tensile tests were performed on specimens extracted from thin die-cast AM60B magnesium alloy plates at room temperature condition, in order to characterize the alloy's basic mechanical properties. The response of the alloy was also studied under elevated temperature. The fatigue tests were

conducted at a stress ratio of R=0.1 at 30 Hz frequency, at both room and elevated temperatures. As well, fatigue crack growth rates (FCGR) were recorded under the above mentioned conditions, and under different stress ratios. The objective was to determine the growth rate at various stress ratios under the same loading frequency, thereby examining the influence of the stress ratio on fatigue life and crack growth rate of the alloy. The analytical models used were firstly the Paris model, followed by the Walker model, in order to characterize the stress ratio's effect. LEFM analyses were conducted for different crack lengths. The assessments of the FCGR of AM60B magnesium alloy, using the above-mentioned models, were carried out using the NISA/ENDURE (Troy, U.S.A.) finite element codes and fatigue analysis.

3.2 MATERIAL AND COMPOSITIONS

Most commercial Mg alloys contain 2-9 wt% aluminum. Under equilibrium conditions, the cast Mg-alloy should solidify as a single phase α-Mg solid solution and further cooling should lead to the solid state precipitation of β-$Mg_{17}Al_{12}$ within the α-grains (Wang & Fan, 2006). The presence of the brittle eutectic phase $Mg_{17}Al_{12}$ affects mainly the mechanical properties of cast Mg alloys (Kleiner et al., 2002). For this study, test specimens were extracted from die-cast AM60B Mg alloy plates provided by the Meridian Technologies Inc. (Strathroy, Ontario). The chemical composition of the alloy is shown in Table 3.1.

Energy dispersive X-ray analysis (EDS) had also been done for the different phases of the AM60B magnesium alloy. The outcomes are given in Tables of 3.2-3.4, along with the SEM images shown in Figures 3.1 and 3.2, which represent a general view of the microstructure of different phases of AM60B alloy. As seen, the weight percentage of the Al element in α-Mg phase is greater than the other phases.

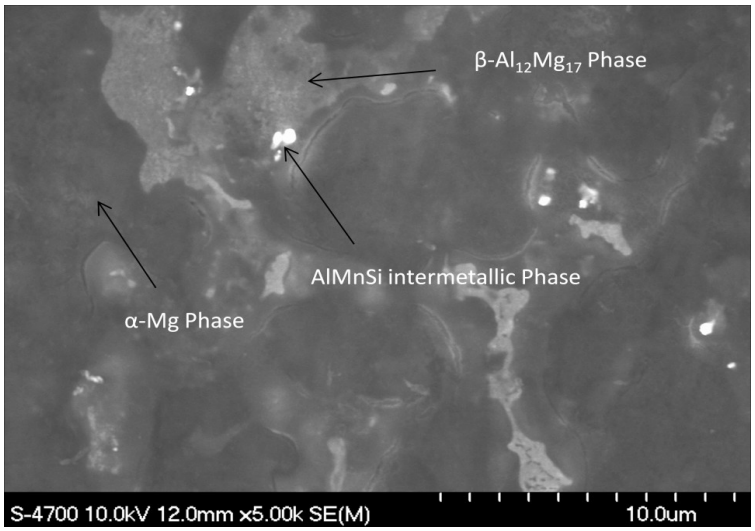

Figure 3.1 Different phases of AM60B magnesium alloy.

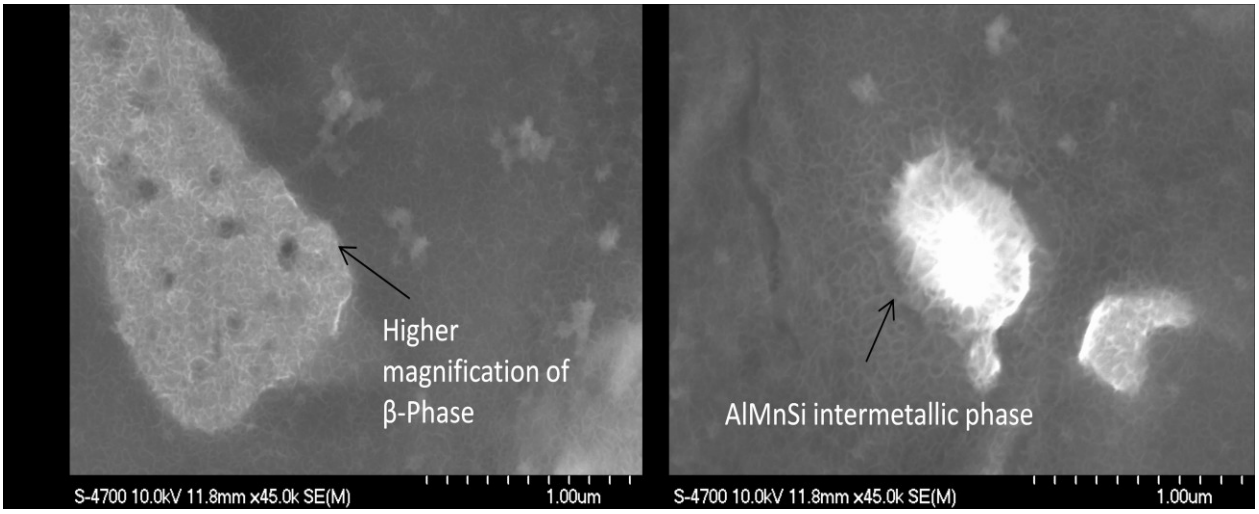

Figure 3.2 SEM images, showing β-phase and Mn-rich intermettalic phase of AM60B magnesium alloy in higher magnification.

Table 3.1 Composition of cast AM60B magnesium alloy in weight %.

Alloy	Al	Mn	Si	Zn	Cu	Fe	Ni	Other	Mg
Cast AM60B	5.5-6.5	0.25 Min	0.10 Max	0.22 Max	0.010 Max	0.005 Max	0.002 Max	0.003 (Total)	Bal.

Table 3.2 EDS elemental analysis of α-Mg phase.

Alloy	C	O	Mg	Al	Total
Weight%	4.21	12.67	72.49	10.63	100.00
Atomic%	7.77	17.53	65.99	8.72	100.00

Table 3.3 EDS elemental analysis of β-phase.

Alloy	C	O	Mg	Al	Total
Weight%	2.32	6.10	68.76	22.83	100.00
Atomic%	4.54	8.97	66.57	19.92	100.00

Table 3.4 EDS elemental analysis of Mn rich intermettalic phase.

Alloy	C	O	Mg	Al	Si	Mn	Total
Weight%	5.28	27.01	45.69	17.72	0.56	3.73	100.00
Atomic%	9.25	35.53	39.55	13.82	0.42	1.43	100.00

3.3 EXPERIMENTAL PROCEDURES

3.3.1 Specimens and Test Set Up

Flat dog-bone shaped tensile and fatigue specimens were extracted from the plates according to ASTM standard E-8M, (Figure 3.3 (a)) and E-466 (Figure 3.3 (b)), respectively, for the static and cyclic tests [(ASTM E-8M, 2003) and (ASTM E-466, 2003)].

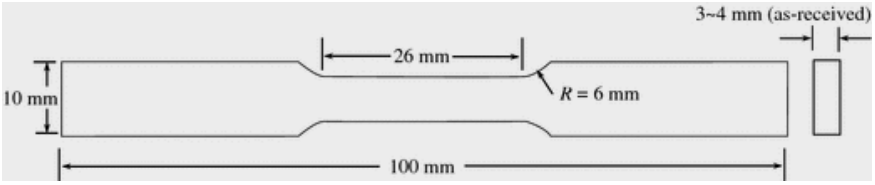

(a)

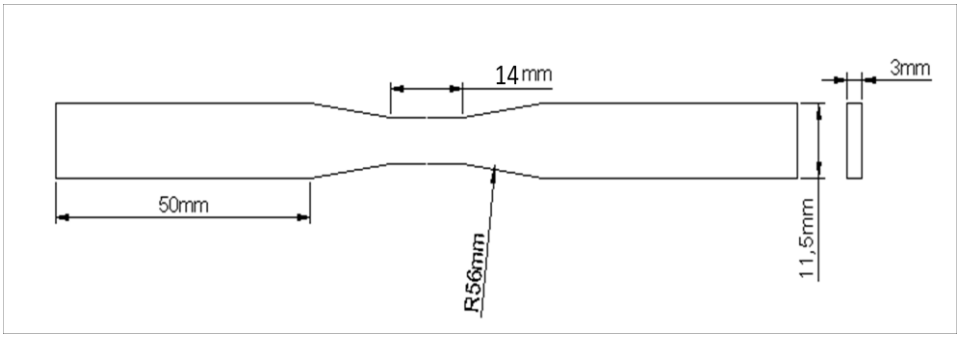

(b)

Figure 3.3 (a) ASTM standard E8M, tensile specimen (ASTM E-8M, 2003); (b) E-466, fatigue specimen (ASTM E-466, 2003).

The specimens were prepared with proper surface finishing operation and the damaged metal on the machined surface was removed by grinding and polishing. The mechanical properties of the alloy were measured by uniaxial tensile test following ASTM E8. Monotonic and cyclic tests were conducted in a servo-hydraulic Instron 8501 machine at room and elevated temperature of 80°Celsius with the Test Star control system (Instron, Norwood, MA), as shown in Figure 3.4(a). For the cyclic testing, five stress amplitude values were applied (i.e. 75-115 MPa, with 10 MPa increment). All fatigue tests were load controlled at a stress ratio R=0.1 [(Wang & Fan, 2006), (Li & Zhang, 2001), (Mann, 2007), and (Wang & Fan, 2004)]. An Instron extensometer was used to record the

specimen's deformation within the gauge length (hence, the strain) during the static tests. A ZBD-104 environmental chamber (as shown in Figure 3.4(b)), manufactured by the Associated Environmental System (Ayer, MA) was used for fatigue tests at elevated temperature. Both an optical microscope and a scanning electron microscopy (SEM) (Hitachi, U.S.A) were used to examine voids and other possible crack initiation sites and microstructures.

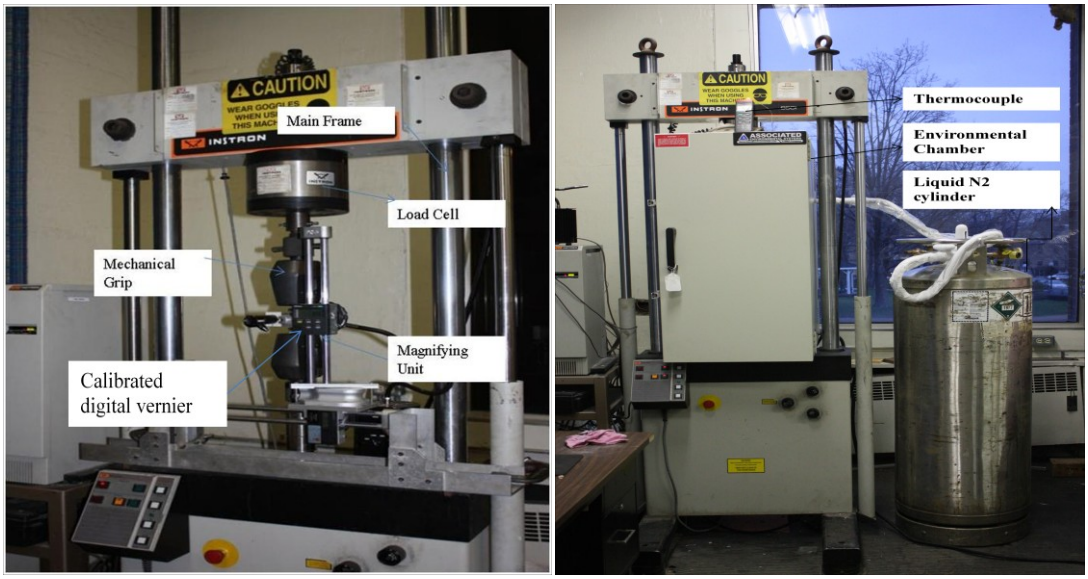

(a) (b)

Figure 3.4 Experimental setup of fatigue crack propagation test (a) at room temperature; (b) at elevated temperature.

3.3.2 Fatigue Crack Propagation Tests

The single edge crack flat specimen geometry was used for the fatigue crack growth tests. The specimens were prepared according to the ASTM E647 standard. The fatigue crack propagation cyclic testing was conducted using the same test machine and control system. The tests were performed under load controll at stress ratios R= 0, 0.1 and 0.2, with the maximum stress value of 80 MPa and frequency of 30 Hz. The incremental lengths of fatigue cracks were measured directly with a calibrated digital Vernier attached to a microscope unit, as shown in Fig. 3.4(a). The specimens were first notched by a jeweller's saw, and subsequently fatigue pre-cracked to introduce a sharp initial crack for the actual fatigue crack growth test. Once the fatigue pre-crack was formed, extension of

the growing crack was recorded as a function of crack length increment and the associated number of cycles. The recording was continued until the specimen had failed. The crack growth length, *a*, versus number of cycles, *N,* curve was plotted for each specimen, which was subsequently post-processed to generate the da/dN versus ΔK curve [(Anderson, 2000) and (Broek, 2001)].

3.4 RESULTS AND DISCUSSION

3.4.1. Static (monotonic) Tension Tests

Figure 3.5 shows the stress versus strain relationship of HPDC AM60B magnesium alloy generated from the tension test data. The average yield strength of the material was determined to be 145 MPa. The variation in the plastic region and ultimate tensile strength is due to large variation in porosity, as determined by the optical and SEM images. The average elongation at fracture was found to be approximately 6.6%. True stress and true strain were calculated by the equations as below.

$$\varepsilon_{true} = ln(1 + \varepsilon_{Engineering}) \quad (3\text{-}2)$$

$$\sigma_{true} = \sigma_{Engineering}(1 + \varepsilon_{Engineering}) \quad (3\text{-}3)$$

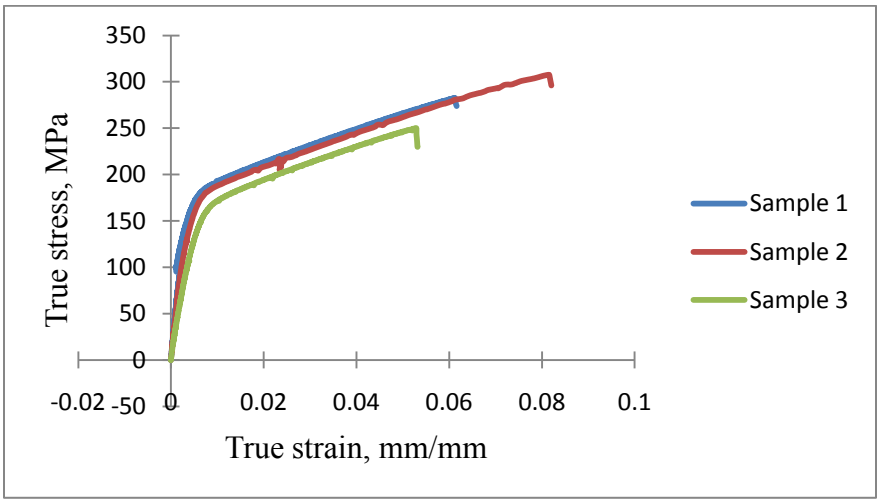

Figure 3.5 Tensile stress-strain curve for HPDC AM60B magnesium alloy.

3.4.2. Fatigue Tests

3.4.2.1. Influence of Elevated Temperature on Fatigue Response of AM60B Magnesium Alloy

A run out cycle limit of 10^6 at stress level 75 MPa was found for all specimens tested at both room and elevated temperatures. Results indicated that there was no significant difference in the number of cycles to failure between room and elevated temperatures at a stress level of 85 MPa, as is illustrated in the respective S-N curves in Figures 3.6 and 3.7. It is concluded that at the lower stress levels the effect of the elevated temperature (i.e. 80° C) on fatigue life of AM60B magnesium alloy is not significant. At high stress levels of 95, 105 and 115MPa, however, the above influence was more pronounced as can be seen in Figures 3.6 and 3.7.

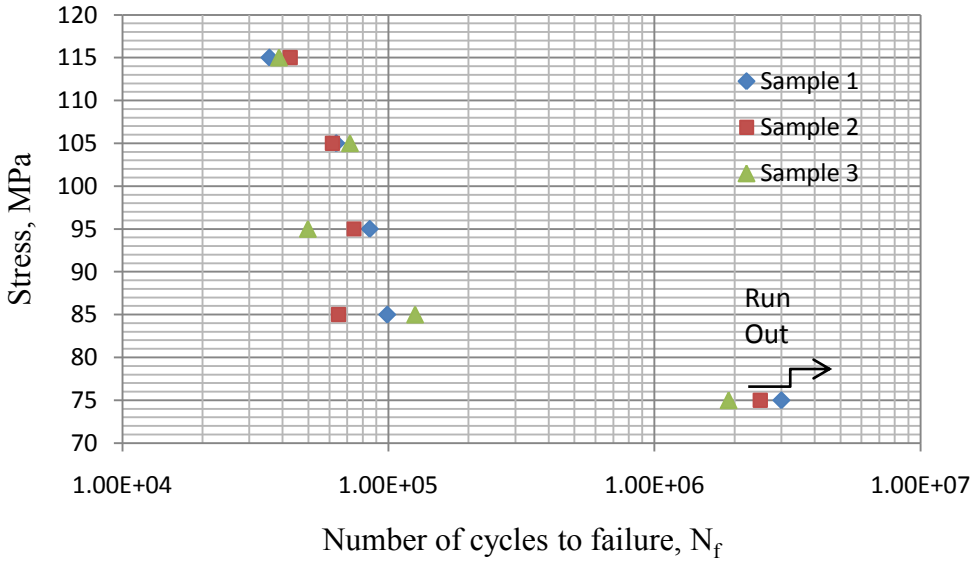

Figure 3.6 Plot of stress vs. number of cycles at room temperature

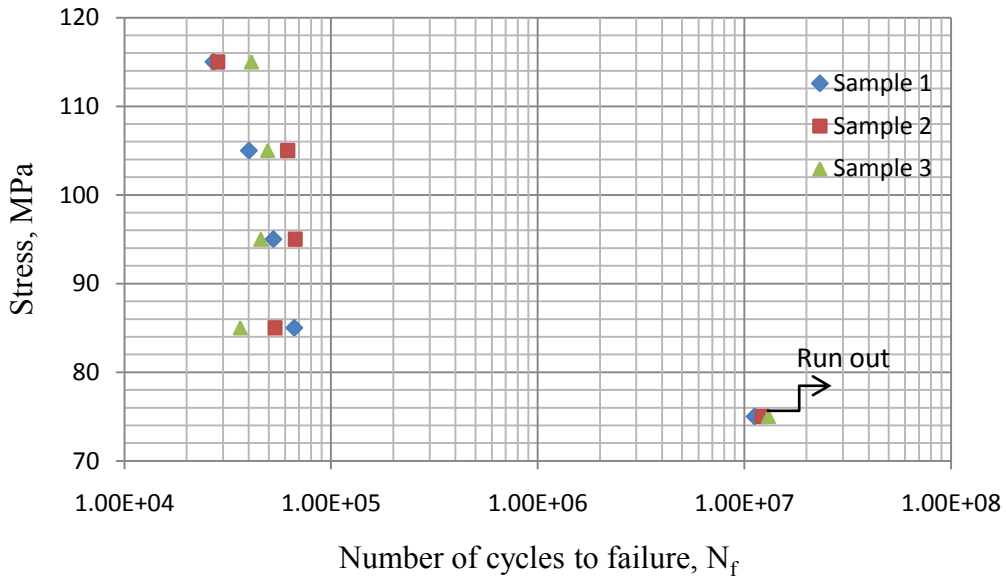

Figure 3.7 Plot of stress vs. number of cycles at 80°C temperature.

Fractography analysis was conducted to further characterize the fracture behavior of die-cast AM60B magnesium alloy. As seen in Figure 3.8, it can be identified that the expansion of voids creates micro-cracks, facilitating the subsequent crack propagation. The small fatigue crack growth path at the elevated temperature is different from that at room temperature. At elevated temperature, huge segregation of β-$Mg_{17}Al_{12}$ occurs in the vicinity of the void's boundary; this is believed to be due to the change in brittle nature of the hard β-$Mg_{17}Al_{12}$. Moreover, the interaction between two adjacent pores for creating a cavity is more significant, as identified for specimens tested at the elevated temperature. In contrast, at room temperature, even at high stress level, no such segregation of β-$Mg_{17}Al_{12}$ could be observed (see Figure 3.8).

Figure 3.8 Micrograph of fatigue specimen at high stress level (95-115 MPa) at room temperature.

The crack tip stress intensity factor is lower at lower stress levels; as a result the lower driving force created at the crack tip cannot cleave the microstructure. Indeed, at lower stress and elevated temperature, micro-cracks propagate with repeated sharpening and blunting; and as a result, no cleavage fracture occurs. Comparison of the void boundary, shown in Figure 3.8 (for specimens tested at room temperature), and that tested at elevated temperature (Figures 3.9 and 3.10), illustrates that β-$Mg_{17}Al_{12}$ segregation occurs at the elevated temperature (evident by the white spots visible around the pore in Figure 3.10). However, at high stress level, the growth behavior of these small fatigue cracks indicates that many α-Mg grains were cleaved along the crack growth path at the elevated temperature, regardless of the stress level; this can be observed through the SEM images shown in Figure 3.11. The main reason is postulated to be due to the variation in brittleness of the β particles at the elevated temperature. Therefore, the fatigue crack growth rate of a small crack would be faster at elevated temperature than that at room temperature. Consequently, the fatigue life at the elevated temperature is shorter than that at room temperature, as supported by the experimental results.

Another important issue is the presence of the foreign particles. These particles are complex compounds of the alloying elements, like Si and Cu. These particles are used to improve the castability and machinability. First, the large particles are released or break; as a result creating widely spaced holes close to the crack tip. In the final phase, voids are formed within myriads of smaller particles. Subsequently, these voids gradually coalesce

to complete the fracture, as shown in Figure 3.12. Commencement of the small fatigue cracks occur along the interfaces of α-Mg grains, due to plastic slipping of surface grains.

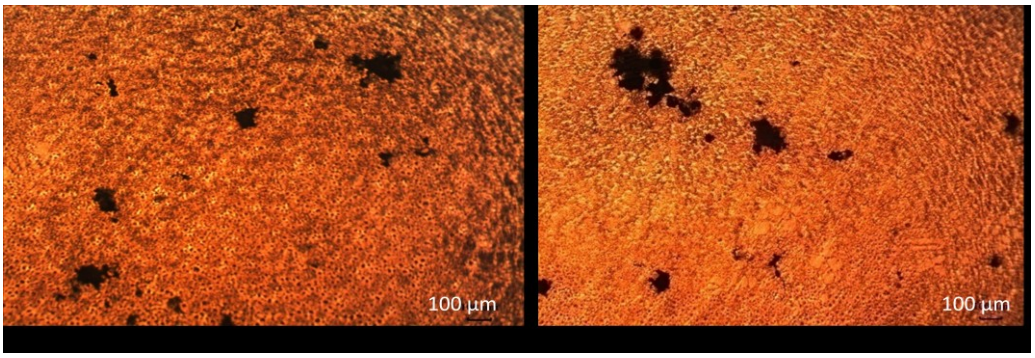

Figure 3. 9 Micrograph of fatigue specimen at low stress level (75-85 MPa) at elevated temperature.

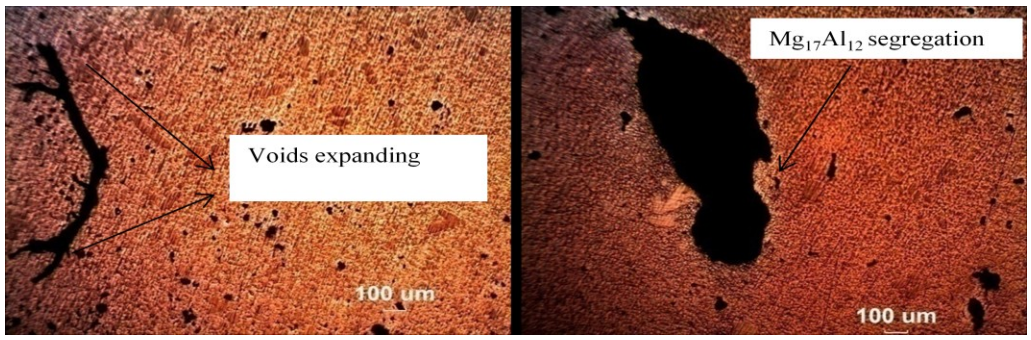

Figure 3.10 Micrograph of fatigue specimen at high stress level (95-115 MPa) at elevated temperature.

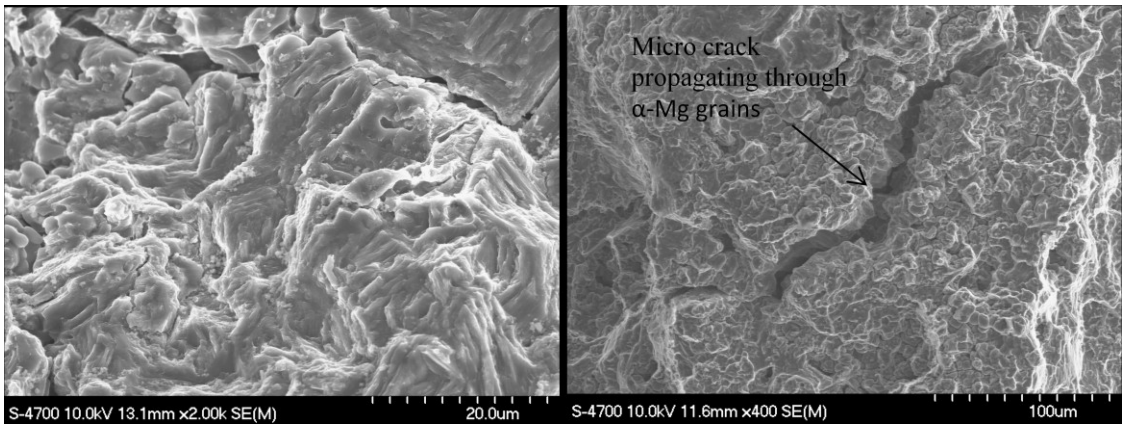

Figure 3.11 SEM images showing crack passing through α-Mg at elevated temperature.

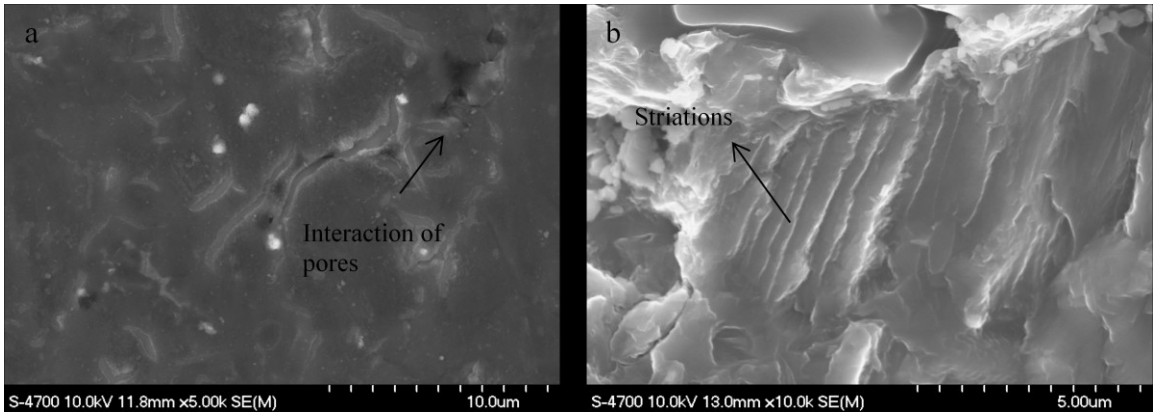

Figure 3.12 (a) SEM image showing interaction of pores and inclusion particles. (b) Striations due to consecutive sharpening and blunting of micro-cracks.

3.4.2.2. Influence of Stress Ratio on Fatigue Characterization of AM60B Magnesium Alloy

Fatigue crack growth rate can be easily evaluated as a function of stress intensity factor range. One of the popular methods to design and analysis fatigue growth rate is the Paris model. The simplest ways to determine the fatigue growth rate by using the Paris model, with both numerical and experimental approaches, are described in Chapter Five.

$$\frac{da}{dN} = C_P(\Delta K)^{m_p} \tag{3-3}$$

In the above equation C_P is the Paris constant, $\frac{da}{dN}$ is the fatigue crack growth rate, ΔK indicates the stress intensity factor range, m_p is the Paris exponent.

The Paris model was extended by Walker [(Anderson, 2000) and (Broek, 2001)] to perform fatigue crack propagation life prediction by accounting for the stress ratio, *R*. By the Walker model, crack propagation rate can be related to the equivalent range of stress intensity factor (SIF), ΔK_{eq} using the following relationship.

$$\frac{da}{dN} = C_P(\Delta K_{eq})^{m_p} \tag{3-4}$$

where,

$$\Delta K_{eq} = \Delta K/(1-R)^{1-\gamma} \tag{3-5}$$

in which: $$\Delta K = Y\Delta\sigma\sqrt{\pi a_{avg}} \quad (3\text{-}6)$$

and $$\left[Y = 0.265(1-\alpha)^4 + \frac{0.857+0.265\alpha}{(1-\alpha)^{3/2}}\right] \quad (3\text{-}7)$$

In the above equations, Y is the geometric factor, α is the ratio between crack length to width and γ is a material parameter ranging from 0.3 to 0.8 [(Dowling,1998), (Broek, 2001), and (Anderson, 1980)].

It is well established that for a given initial crack size, the fatigue life would be a function of the magnitude of the applied stress and the fracture resistance of the material (Broek, 2001). The procedure therefore entails the evaluation of the stress intensity factor range, ΔK, for a given crack growth rate *da/dN*. The Walker model has been widely used in the aerospace industry, because it is simple to apply, requires only one additional parameter (γ, which is usually assumed to be 0.5), and produces reasonable results for many materials, provided that *R* is not too high.

As stated earlier, at positive stress ratios, the exponent γ usually takes values between 0.3 and 0.8. When, γ=0.3, there would be a strong dependency of FCP to *R*, while γ=0.8 produces a weaker dependence on *R* (Wang & Fan, 2006). The exact value of γ is not known for AM60B magnesium alloy at stress ratio of R=0.1; usually γ=0.5 is assumed, which is known to produce a reasonable estimate [(Wang & Fan, 2006) and (Mann, 2007)].

In order to determine the influence of the stress ratio, the test results are plotted in the format shown in Figures 3.13-3.15. The crack growth rates for *R*=0.1 and 0.2 are extrapolated based on the test data for *R*=0, using the Walker equation. The comparison of the analytical and experimental values for the two stress ratios are also shown in Figures 3.13-3.15. As can be seen, the FCP rate increases as a function of the stress ratio. This variation is quite significant when crack length tends to grow to a critical crack length, thereby imposing large stress intensity factors. The results clearly show that the crack growth rate is dependent on the stress ratio and this effect would be stronger at a larger stress ratio. The above analytical and experimental results were also compared

with the predictions by the finite element analysis as shown in Figure 3.15. Although there are some differences among the experimental results, and those obtained by the analytical and finite element method in the region of lower growth rate, nevertheless a reasonable overall agreement is obtained. For example for R= 0.1, the initial growth rate was found be 2.52×10^{-07}m/cycle experimentally, which is compared to 1.81×10^{-07}m/cycle and 3.8×10^{-07}m/cycle obtained by the analytical and finite element methods, respectively. On the other hand, the final growth rate was found to be 6.80×10^{-06} m/cycle, 7.40×10^{-06} m/cycle and 6.46×10^{-06} m/cycle, respectfully, obtained experimentally, analytically and numerically, showing much better corroboration.

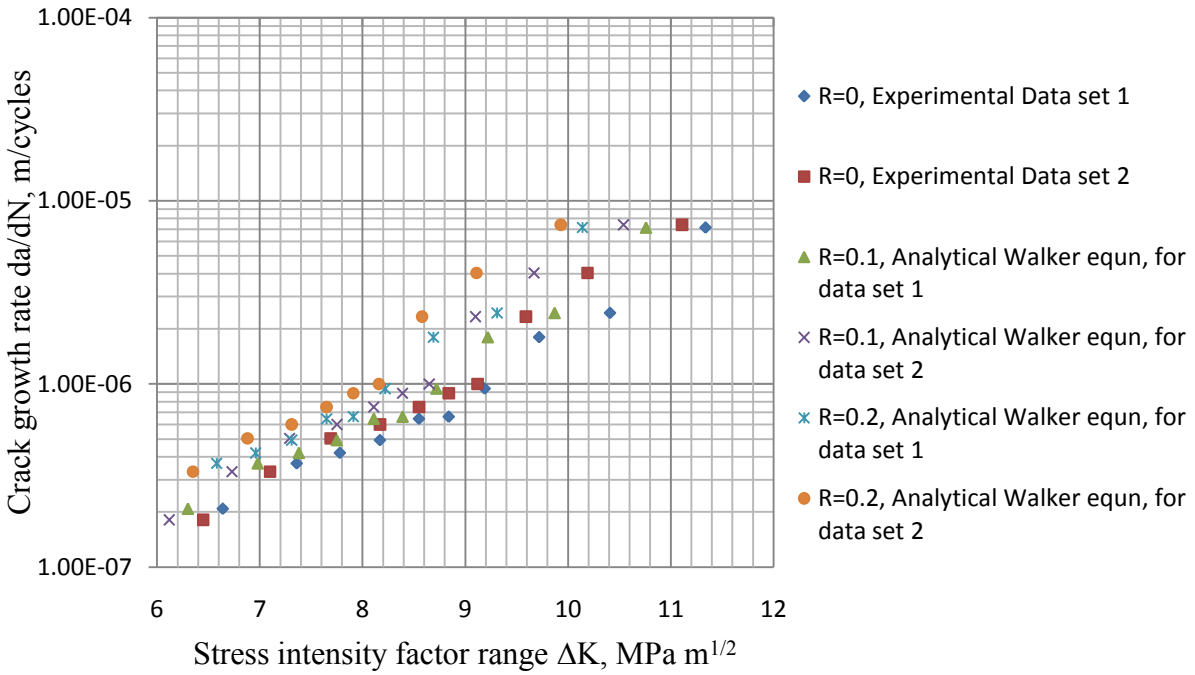

Figure 3.13 Fatigue crack growth rate calculated by the Walker model, based on the experimental data for R=0.

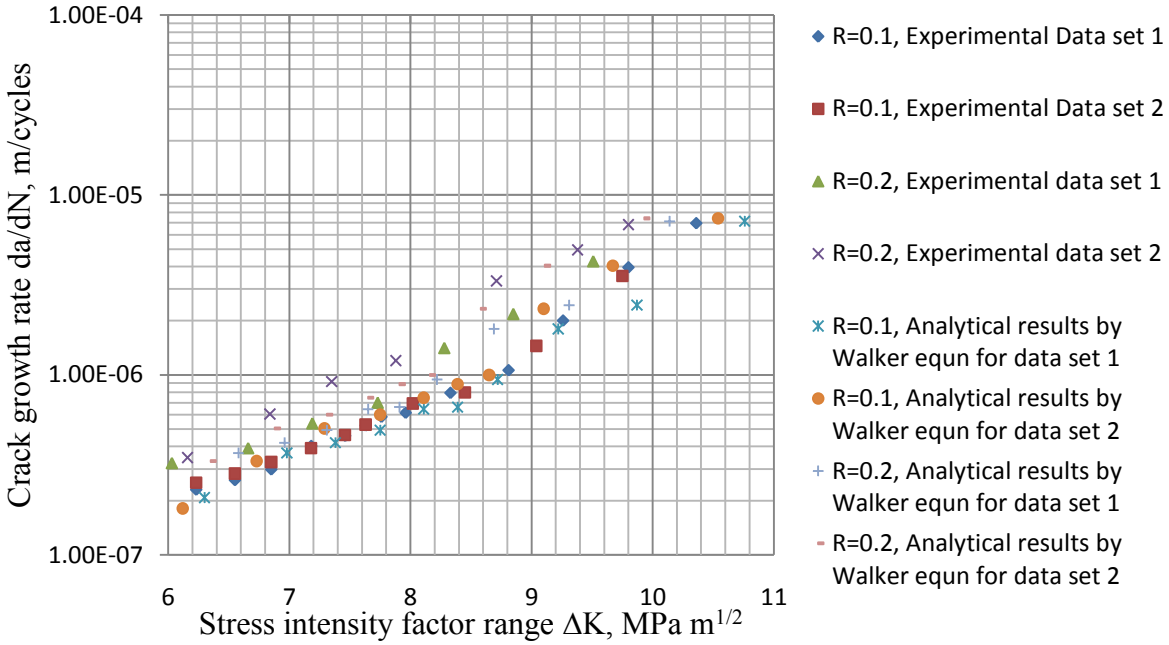

Figure 3.14 Plot of ΔK vs. da/dN at R=0.1 and R=0.2 obtained experimentally and analytically.

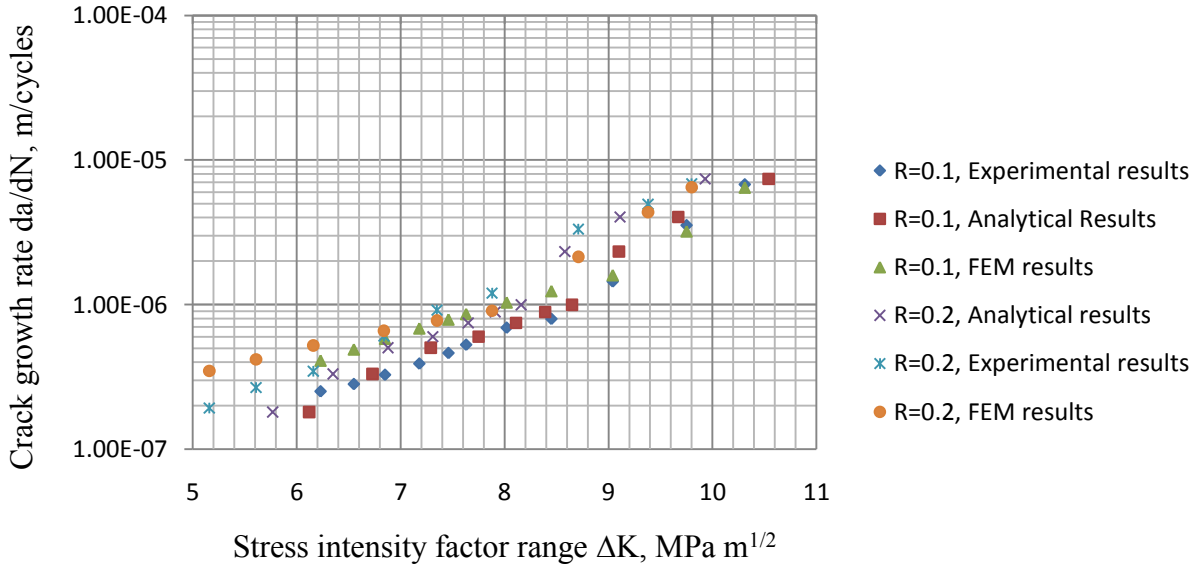

Figure 3.15 FCGR (Fatigue crack growth rates) with consideration of the mean stress (analytical, experimental and FEM).

In consideration of the SEM images of fracture surfaces shown in Figure 3.16, significant serrated and faceted surfaces are seen in the region further away from initiation zone. These serrated and faceted surfaces indicate that the zone belongs to the propagation zone at the micro level. Moreover, the area hosting these surfaces are larger in the specimens that have been subject to larger stresses, as shown in Figure 3.16(b), as opposed to that shown for the lower stress level in Figure 3.16(a). Larger and more pronounced microcracks were observed in the SEM mages of specimens failed at the higher stress ratio, which is clearly observed from Figure 3.16 (c,d,e and f). Shrinkage porosity was also observed, as shown in Figure 3.17, which is believed to have also been responsible in expediting the crack propagation rate.

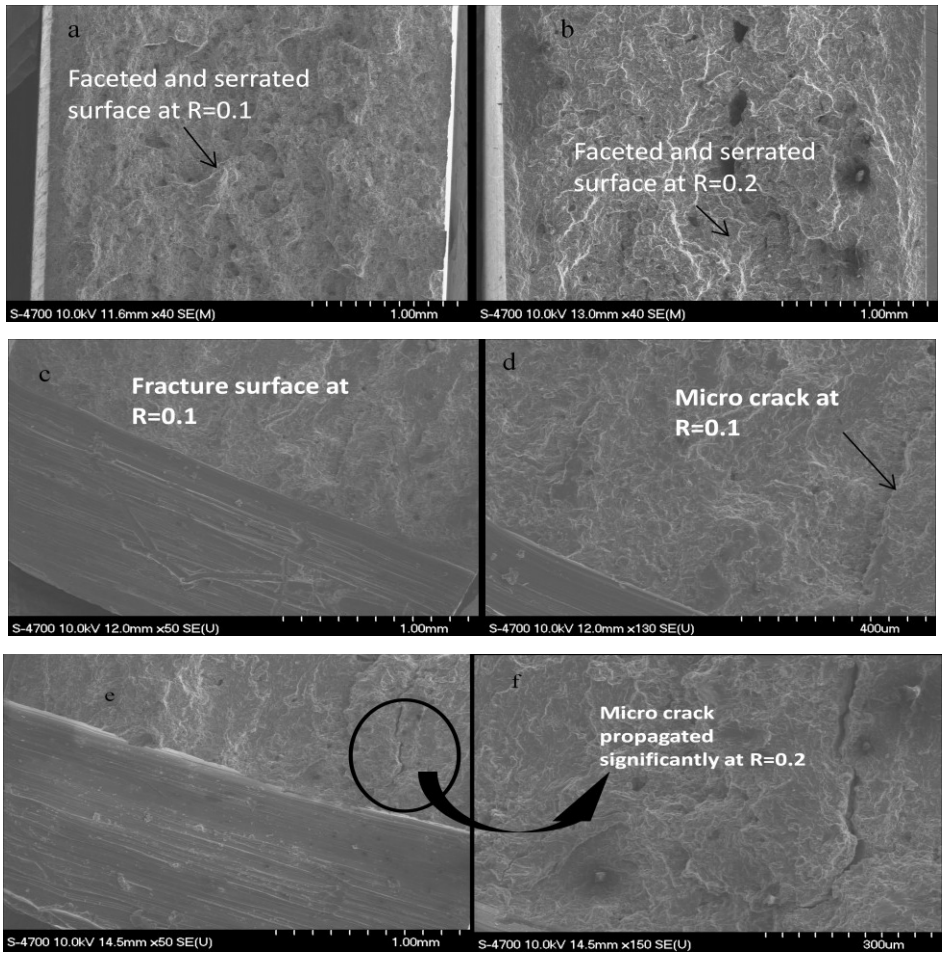

Figure 3.16 SEM images showing serrated and faceted surface at (a) at R=0.1 ;(b) at R=0.2; (c, d, e and f) micro crack found at both stress ratios.

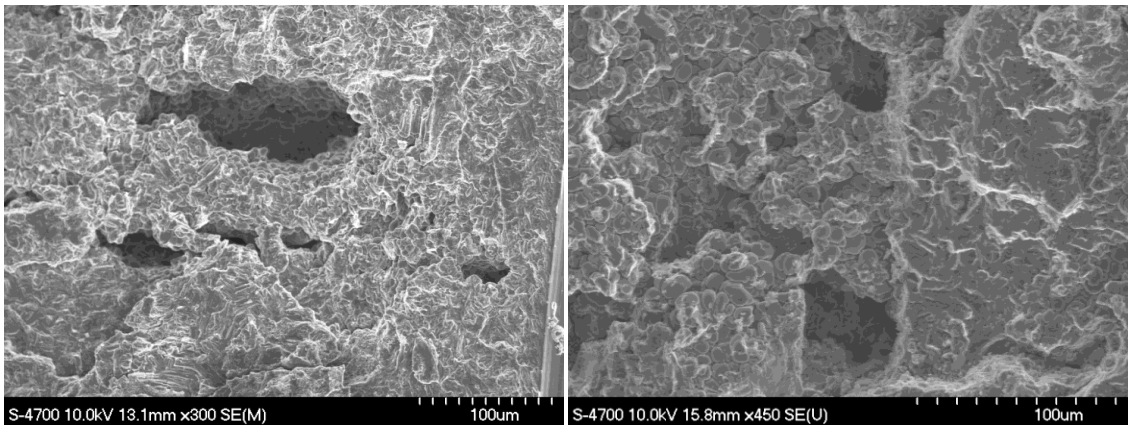

Figure 3.17 Shrinkage porosities found in the failure surfaces.

3.5 CONCLUSION

Experimental, analytical and computational investigations were conducted with the aim of characterizing and predicting the fatigue response and crack growth rate of AM60B magnesium alloy at room and elevated temperatures. The influence of the stress ratio was also a primary objective of the investigation.

It is postulated that cracks are initiated in the alloy mainly due to the internal discontinuities due to the presence of porosity, followed by the final fracture resulting from the growth and coalescence of the cracks, as seen in the SEM images.

It was observed that at elevated temperature of 80° Celsius, the fatigue life of AM60B magnesium alloy decreased. The decrease was not significant at low stress levels. The initiation of small fatigue cracks generally occurred along the interfaces of the α-Mg grains, due to the micro-mechanism of the accumulative plastic slipping of surface grains (α-Mg) and the deformation mismatch of the two phases at room temperature. However, the small fatigue cracks mainly cleaved the α-Mg grains at the elevated temperature. Large segregation of brittle eutectic β-$Mg_{17}Al_{12}$ along the grain boundaries also caused the cleavage of the α-Mg grains at the elevated temperature. At the elevated temperature, the small fatigue cracks propagated through the α-Mg grains, since these regions were softened due to the high temperature.

Walker's model was effectively used for predicting the crack growth rate at various stress ratios of AM60B magnesium alloy based on the data at R=0 baseline. The growth rate was found to increase as stress ratio increased from R=0.1 to 0.2. At ΔK= 9.1 MPa $m^{1/2}$ for stress ratio R=0.1, the growth rate is $1.45x10^{-06}$ m/cycle. On the other hand, at the same stress intensity factor, for R=0.2, the growth rate was found $4.00x10^{-06}$ m/cycle.

The experimental and analytical results were also very close to those predicted by our finite element analysis. Further experimental results at higher stresses are required to further establish the concluded trend.

The observed variation in the fatigue crack growth behavior is strongly influenced by the variation in porosity size and distribution within each specimen. Consequently, further studies are needed to clarify the crack propagation behavior at the positive R regions.

3.6 ACKNOWLEDGEMENT

This research is carried out with the financial support provided by AUT021 Network of Centers of Excellence, an automotive research and development program focusing on issues relating to the automobile in the 21st century. We are indebted to AUTO 21 for the financial support and IRM (The Institute for Research in Materials, Dalhousie University) for using SEM.

3.7 REFERENCES

Anderson, T.L. (2000). Fracture mechanics: Fundamentals and applications, second edition. *CRC Press, Inc*. FL, USA. pp. 573-577.

ASTM E-8M standard, (2003). Test methods of tension testing of metallic materials [metric]. Annual book of ASTM: volume 03.01, *American Society of Metals*. Metals Park, Ohio. pp. 83-104.

ASTM E-466 standard, (2003). Standard practice for conducting force controlled constant amplitude axial fatigue tests of metallic materials. *Annual book of ASTM*: Volume 03.01, *American Society of Metals*. Metals Park, Ohio. pp. 515-519.

ASTM E-647 standard, (1996). Standard practice for conducting force controlled constant amplitude axial fatigue tests of metallic materials. *Annual book of ASTM*: Volume 03.01. Metals Park, Ohio.

Broek, D. (2001). The practical use of fracture mechanics. *FractuREsearch Inc*. Galena, OH, USA. pp. 44-86.

Dowling, N. (1998). Mechanical behavior of materials. *Prentice-Hall: Inc*. New Jersey, USA.

Grinberg, N., Serdyuk, V., & Ostapenko, I. (1977). Features of fatigue failure in magnesium alloy MA12 in air and in vacuum. *Mechanics of Materials 6*, pp. 61-66.

Ishihara, S., McEvily, A., Sato, M., Taniguchi, K., & Goshima, T. (2009). The effect of load ratio on fatigue life and crack propagation behavior of an extruded magnesium alloy. *International Journal of Fatigue 31*, pp. 1788-1794.

Kleiner, S., Beffort, O., Wahlen, A., & Uggowitzer, P. (2002). Microstructure and mechanical properties of squeeze cast and semisolid cast Mg-Al alloys. *Journal of Light Metals 2*, pp. 277-80.

Koch, T.A. (2004). Fatigue properties of high pressure die cast magnesium AM 60. M.A.Sc. Thesis, Dalhousie University, Department of Metturgical Engineering. Halifax, Nova Scotia, Canada.

Li, W., & Zhang, X. (2001). Investigation of initiation and growth behavior of short fatigue emanating from a single edge notch specimen using in situ SEM6. *Material Science of Engineering 318*, pp. 129-36.

Lu, Y. (2008). Fatigue properties of high pressure die cast magnesium AM 60B alloy using experimental and computational investigations. PhD. Thesis, Dalhousie University, Materials Engineering. Halifax, Nova Scotia, Canada.

Lu, Y., Taheri, F., & Gharghouri, M. (2008a). Monotonic and cyclic plasticity responses of high pressure die cast AM60B magnesium alloy. To appear in Strain.

Lu, Y., Taheri, F., & Gharghouri, M. (2008b). Study of fatigue crack incubation and propagation mechanisms in a HPDC AM60B magnesium alloy. *Journal of Alloys and Compound* 466, pp. 214-227.

Mann, T. (2007). The influence of mean stress on fatigue crack propagation in aluminum alloy. *International Journal of Fatigue* 29, pp. 1393–1401.

Stephens, R., Fatemi, A., Stephens, R., & Fuchs, H. (1980). Metal Fatigue in Engineering. John *Wiley & Sons, Inc.*, NJ, USA.

Wang, X.S. & Fan, J.H. (2006). An evaluation on the growth rate of small fatigue cracks in cast AM50 magnesium alloy at different temperatures in vacuum conditions. *International Journal of Fatigue 28*, pp. 79-86.

Wang, X.S. & Fan, J.H. (2004). SEM online investigation of fatigue crack initiation and propagation in notched cast magnesium specimens. *Journal of Material Science 39(7)*, pp. 2617-20.

Zenga, R., Xub, Y., & Hanb, E. (2009). Fatigue crack propagation behavior of an as-extruded magnesium alloy AZ80. *Materials Science and Engineering* A 509, pp. 1-7.

CHAPTER 4: FATIGUE AND FRACTURE CHARACTERIZATION OF HPDC AM60B MAGNESIUM ALLOY AT LOW TEMPERATURE

Md. Nur Hossain and Dr. Farid Taheri

Publication Status: Submitted to Journal of Materials Engineering & Performance

4.0 ABSTRACT

An investigation of the fatigue and fracture characterization of the high pressure die cast (HPDC) AM60B magnesium alloy at -40°C temperature was conducted by means of the constant load amplitude fatigue test. The results demonstrated that low temperature had a significant influence on alloy's fatigue life; the life increased at -40°C temperature as compared to that at room temperature. The fracture surfaces of the tested specimens were observed under a scanning electron microscope (SEM) to further understand the fracture phenomenon at low temperature.

Keywords AM60B magnesium alloy; Stress ratio; S-N curves; SEM (Scanning Electron Microscope); Ductile fracture; Brittle fracture.

4.1 INTRODUCTION

Magnesium alloys are increasingly being utilized as one of the important structural materials due to their relatively low weight and high specific strengths. Nowadays, the automotive industry is widely using magnesium alloys as automobile components, resulting in weight saving for car bodies, thus a reduction in fuel consumption. Among all other magnesium alloys, cast magnesium alloys are finding incremental use in the automotive industries. The ongoing interest in the use of cast magnesium alloys in the automotive industries has recently triggered substantial research efforts, mainly focusing on characterization of the structural properties of the alloys (Wang & Fan, 2006). Most magnesium applications presently used in the automotive industry are in the form of high pressure die cast (HPDC) alloys. Applications of HPDC AM60B magnesium alloy, such as those in front and support assemblies, steering wheel armature, instrument panel and steering column support brackets, play a vital role in the automotive industry (Sun et al., 2007). The more significant use of the alloy in different fields demands knowledge of its fatigue response. However, relatively low fatigue strength under service conditions has been a pressing issue, restricting the application of magnesium alloys to low-stress designs [(Horstemeyer et al., 2004) and (Zenner & Renner, 2002)].

In this study, AM60B alloy, which has been characterized as an alloy with outstanding ductility and energy absorbing properties, combined with good strength, less weight and castability, is considered. Materials, especially those with relatively low fracture toughness, could fail at stress levels below their ultimate strength. It has been indicated that the porosity level of components can influence a material's mechanical properties, such as the ultimate tensile strength (UTS), yield strength (YS), and elongation [(Gjestland et al., 2003) and (Zhou, 2004)].

In recent years, some studies have been performed on fatigue characterization of various die-cast magnesium alloys. However, a very limited number of investigations have been conducted on fatigue characterization of HPDC magnesium alloys. It should also be noted that the fatigue of HPDC magnesium alloys at low temperature has hardly been studied. The increase in the fatigue strength and endurance limit as a function of

decreasing temperature is a common tendency in some materials (such as for steel alloys). On the other hand, fatigue strength is known to decrease due to increase in the ambient temperature. Koch (2004) also investigated the fatigue limit of HPDC AM60 magnesium alloy. Later Lu (2008) reported the fatigue characterization of HPDC AM60B magnesium alloy at room temperature. However, the last two sets of studies did not investigate the fatigue behavior of the alloy at low temperatures.

Sajuri et al. (2005) studied the effects of humidity and temperature on the fatigue behavior of an extruded AZ61 magnesium alloy. According to their results, it was identified that a significant reduction in fatigue strength was observed with an increase of temperature to 150°C. Venkateswarana et al. (2004) reported the fatigue crack growth behavior of a die-cast AZ91D magnesium alloy. Grinberg et al. (1979) described the effect of low temperature on the fatigue failure of the magnesium alloy MA12. According to Grinberg's results, it was identified that reductions in temperature lead to an increase in fatigue limit. When the temperature was reduced from 20 to -120ºC with identical cyclic loading, the fatigue life of MA12 magnesium alloy was increased due to the crack initiation stage. It takes more loading cycles to initiate the crack.

In the present paper, the fatigue and fracture response of HPDC AM60B magnesium alloy is investigated at low temperature. In this investigation, static tensile tests have been performed on samples obtained from thin die-cast plates, at room temperature condition, in order to gain better understanding of how the material behaves and its mechanical properties; the general temperature response of AM60B magnesium alloy is also studied. The fatigue tests were performed at stress ratio of R=0.1, at 30 Hz frequency, at both room and low temperatures. In addition, the fracture behavior of the HPDC AM60B affected by low temperature, was characterized by using scanning electron microscopy (SEM) fractography. The main objective of this study is to investigate and determine the influence of low temperature on the fatigue and fracture characterization of HPDC AM60B magnesium alloy.

4.2 MATERIAL AND COMPOSITION

Most commercial casting Mg alloys contain 2-9 wt% aluminum. Under equilibrium conditions, the cast Mg alloy should solidify as a single phase α-Mg solid and upon

further cooling, should lead to the solid state precipitation of β-$Mg_{17}Al_{12}$ within the α-grains (Wang & Fan, 2006). The presence of the brittle eutectic phase $Mg_{17}Al_{12}$ affects mainly the mechanical properties of cast Mg alloys (Kleiner et al. 2002). Here for this study, test specimens were extracted from die cast AM60B Mg alloy plates provided by Meridian Technologies Inc. (Strathroy, Ontario). The chemical composition of the alloy is shown in Table 4.1.

Table 4.1 Composition of cast AM60B magnesium alloy in weight %

Alloy	Al	Mn	Si	Zn	Cu	Fe	Ni	Other	Mg
Cast AM60B	5.5-6.5	0.25 Min	0.10 Max	0.22 Max	0.010 Max	0.005 Max	0.002 Max	0.003 (Total)	Bal.

4.3 EXPERIMENTAL PROCEDURES

Flat dog-bone shaped tensile and fatigue specimens were extracted from the plates according to ASTM standard E-8M (Figure 4.1(a)) and E-466 (Figure 4.1(b)), respectively, for static and cyclic tests [(ASTM E-8M, 2003), (ASTM E-466, 2003)]. The samples were prepared with proper surface finishing procedure by using polishing emery papers and then the damaged metal on the machined surface was removed by grinding followed by additional polishing. The mechanical properties of the alloy were measured by uniaxial tensile testing conforming to ASTM E8 (ASTM E-8M, 2003). Monotonic and cyclic testing (at room and low temperature (-40° C) were conducted using a servo-hydraulic Instron 8501 machine controlled with the Test Star system (Figure 4.2 (a)). For the cyclic testing, four stress amplitudes were considered from 85-115 MPa with 10 MPa increments. All fatigue tests were load controlled at a stress ratio of R= 0.1 [(Mann, 2007) and (Wang & Fan, 2004)] with 30 Hz frequency. A standard extensometer was used to record the displacement during the static test. A ZBD-104 environmental chamber (as shown in Figure 4.2(b)), manufactured by the Associated Environmental System (Ayer, MA) was used for fatigue tests at low temperature. This chamber was operated using cryogenic liquid N_2. Optical microscope and SEM was used to examine voids and other possible crack initiation sites and microstructures.

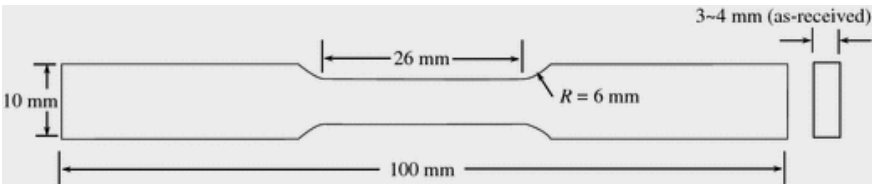

(a)

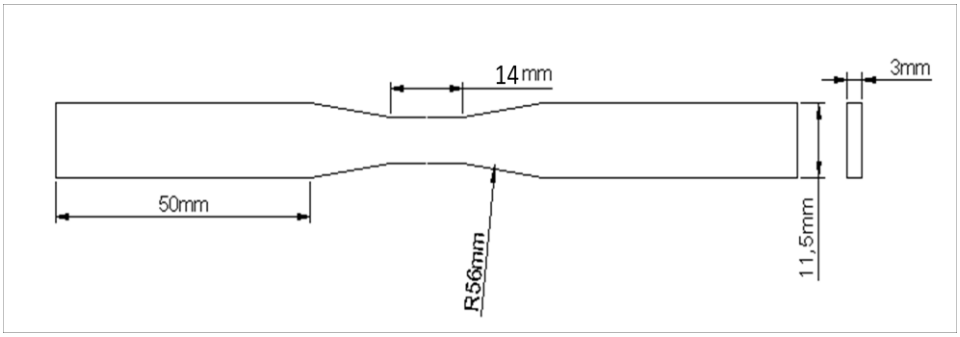

(b)

Figure 4.1 (a) Specifications of ASTM standard E8M tensile specimen [(ASTM E-8M, 2003)]; (b) E-466 fatigue specimen [(ASTM E-466, 2003)].

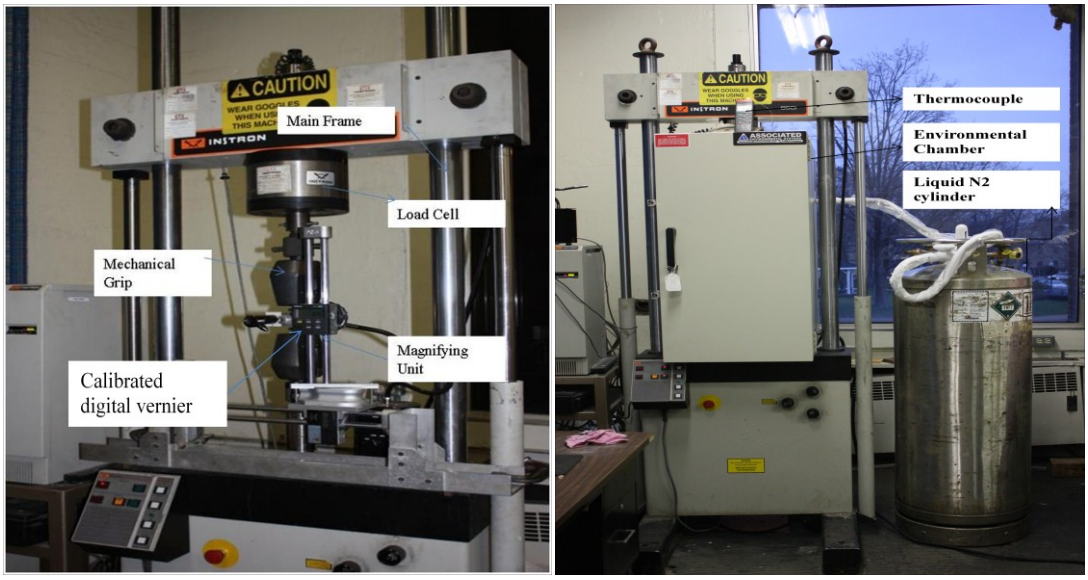

(a) (b)

Figure 4.2 Experimental setup of fatigue test; (a) at room and (b) at low temperature.

4.4 RESULTS AND DISCUSSION

4.4.1 Monotonic Tension Tests

Figure 4.3 shows the stress versus strain relationship from the uniaxial tension tests for HPDC magnesium AM60B alloy. The curves do not show a clear elastic region, indicating that some plastic deformation is taking place. The average value of yield strength of the material was evaluated at 145 MPa. Note that there was a significant variation in the ultimate tensile strength due to large porosity variation as observed in the micrograph and SEM images. True stress and true strain were calculated by the equations as below.

$$\varepsilon_{true} = ln(1 + \varepsilon_{Engineering}) \quad (4\text{-}1)$$

$$\sigma_{true} = \sigma_{Engineering}(1 + \varepsilon_{Engineering}) \quad (4\text{-}2)$$

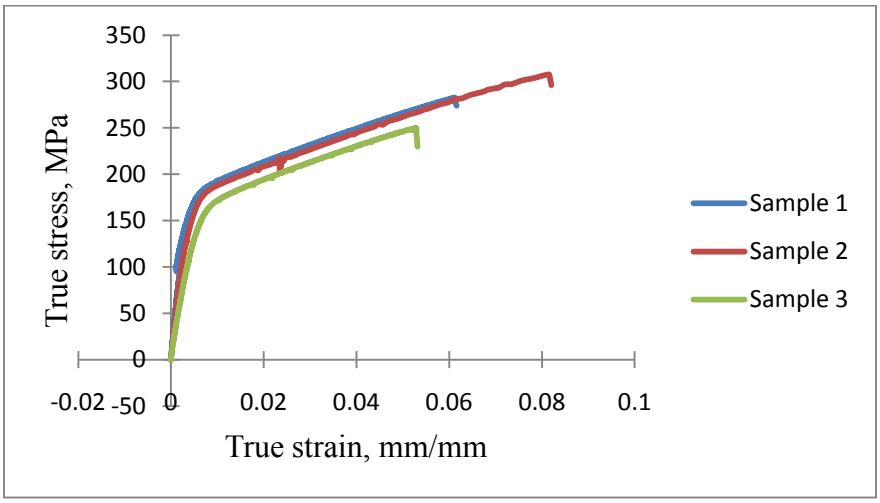

Figure 4.3 Tensile stress-strain curve of HPDC AM60B magnesium alloy.

4.4.2 Fatigue tests

4.4.2.1. Influence of Cold Temperature on Fatigue and Fracture Response of AM60B Magnesium Alloy

Figure 4.4 and 4.5 illustrate the S-N curves plotted from the test results collected at room and cold (-40°C) temperatures respectively. According to the graph, it can be seen that at low temperature, the number of cycles to failure is increased as compared to those tested

at room temperature. This influence is more pronounced at lower stresses than at higher stress values. For example, at a stress value of 85 MPa, it is found that N_f= 98924, 64893 and 125888 for the three specimens tested at room temperature; whereas at cold temperature, for the same stress value, the number of cycles to failure were N_f= 278867, 206107 and 171317. This is almost a doublings of the fatigue life. In other words, at a higher stress value of 115 MPa, the average number of cycles to fatigue failure was found to be 38246 at room temperature, compared to 44192, observed for the specimens tested at low temperature. Again, the difference is large, but not as significant as that at the lower stress value.

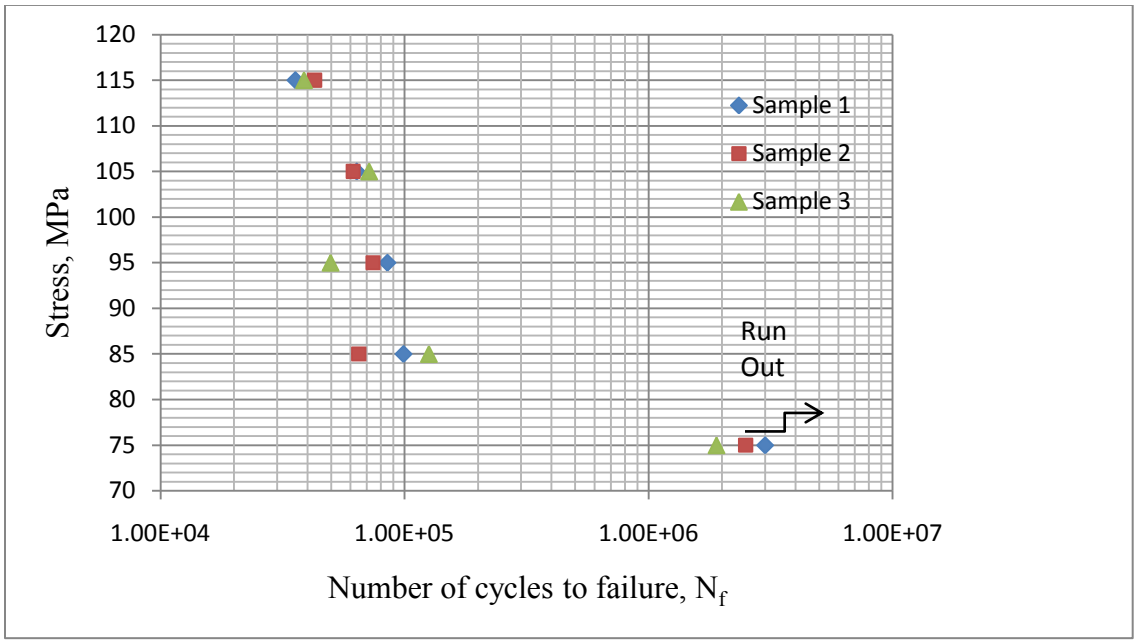

Figure 4.4 Stress vs. number of cycles curve at room temperature

Further insight can be obtained on the fracture behavior of HPDC AM60B magnesium alloy through fractography analysis. Significantly, long fatigue cracks were observed in the SEM images of the whole cross section area taken at lower magnification, for the specimen failed at N_f= 64893, as shown in Figure 4.6(a and b). Whereas short fatigue cracks, with a faceted surface were observed in the SEM images of the specimen failed at N_f= 171317 at low temperature, as shown in Figure 4.6(c and d).

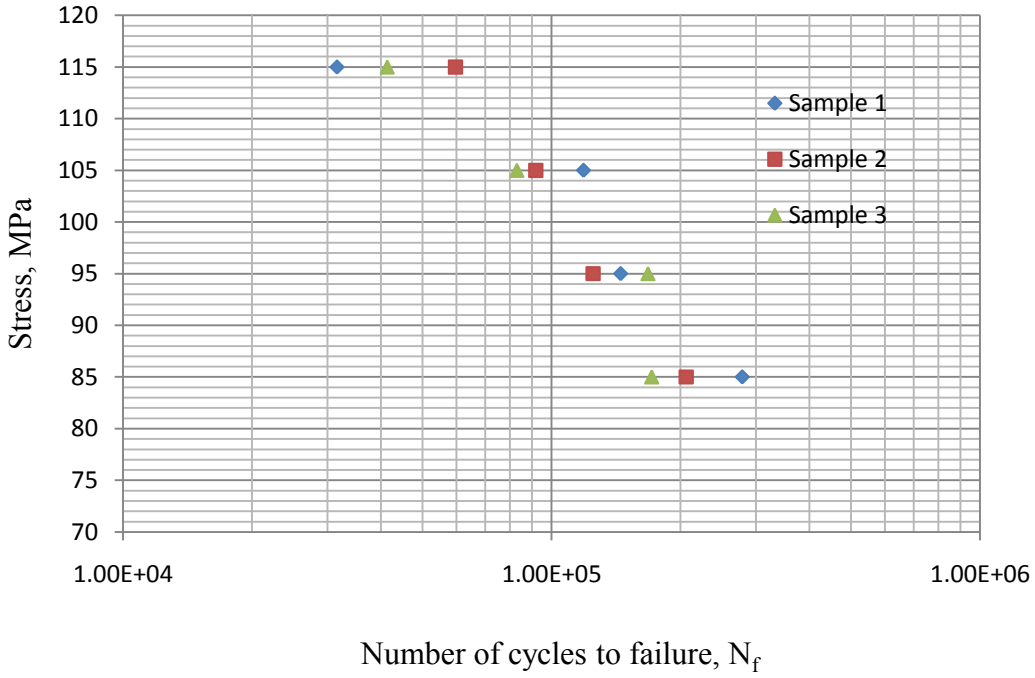

Figure 4.5 Stress vs. number of cycles curve at -40°C temperatures

Figure 4.7 represents the SEM images, under lower magnification, of the fracture surfaces of specimen failed at stress value of 115 MPa at room and low temperatures. Similarly, a significant fracture indication was observed for the case of room temperature. At low temperature, the phases of AM60B magnesium alloy become harder, resulting in mismatch of hardness between the two phases. As a result, the material consumes more loading cycles to reach the critical stress intensity factor at the crack tip. Another anomoly is due to the hard brittle microstructure existing around the voids. The tendency for the crack initiation at the void regions is less in low temperature as opposed to that at room temperature.

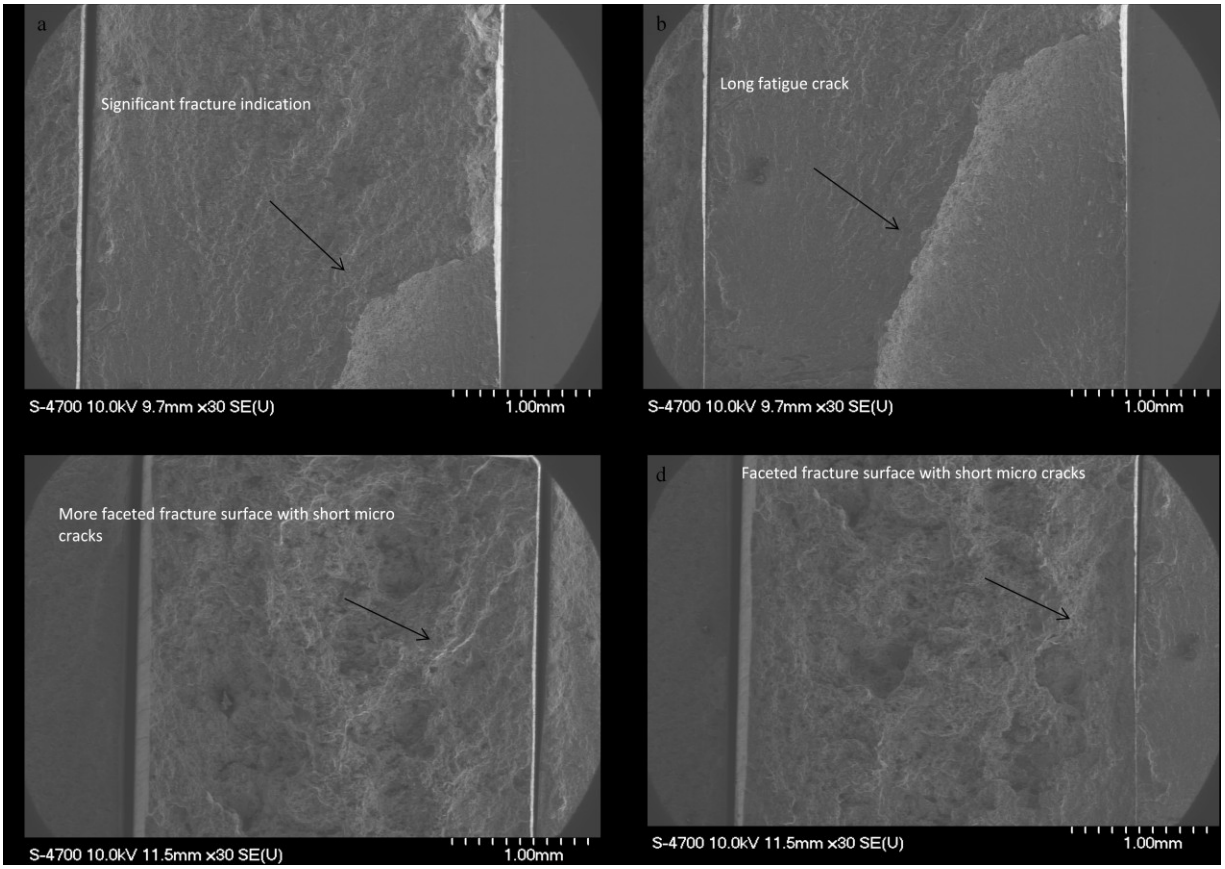

Figure 4.6 Fracture surfaces of the specimens tested at 85 MPa (lower magnification) at room temperature, N_f=64893, (a and b); (c and d) at the room temperature, N_f=171317.

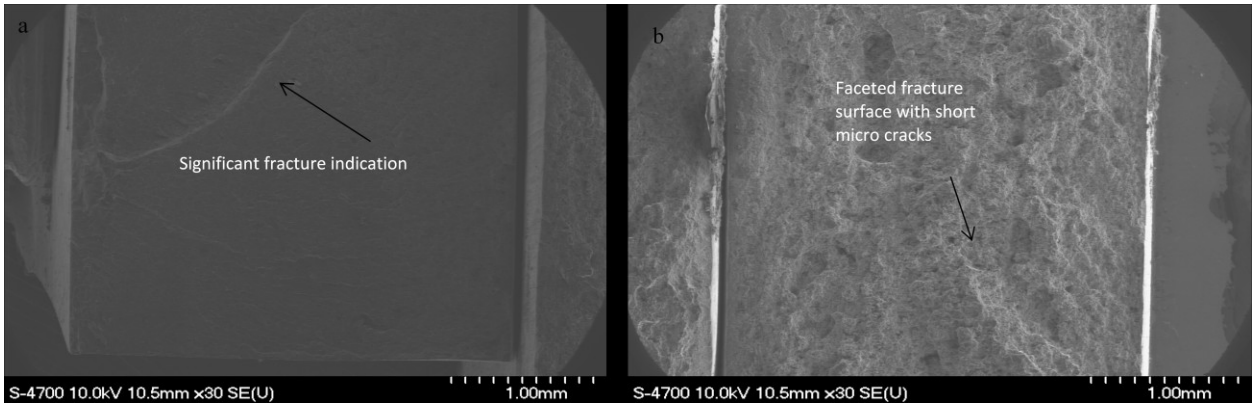

Figure 4.7 Fracture surfaces of the specimens tested at 115 MPa (lower magnification) at room temperature, N_f=38743, (a); (b) at the cold temperature, N_f=59658.

Figures 4.8 and 4.9 illustrate the higher magnification SEM images of fracture surfaces of specimens failed under the lower and higher stress values (i.e. of 85 and 115 MPa), both

at room and low temperatures. Severe fracture was found at room temperature; it is believed this is the reason the material requires less number of cycles to fail, as compared to that at low temperature. Huge striations can be observed in the SEM images of the fracture surfaces of the specimens tested at the room temperature, indicating sharpening and blunting through ductile fracture, as seen in Figure 4.10 (a and b). Smooth pore boundaries can also be identified in the SEM images of fracture surfaces of the specimens tested at the low temperatue, demonstrating less tendency of fracture with microvoid coalescence as seen in the Figure 4.10 (c and d). Shrinkage porosity was also found as shown in Figure 4.11; it is believed these are the agents responsible for acceleration in the crack propagation rate.

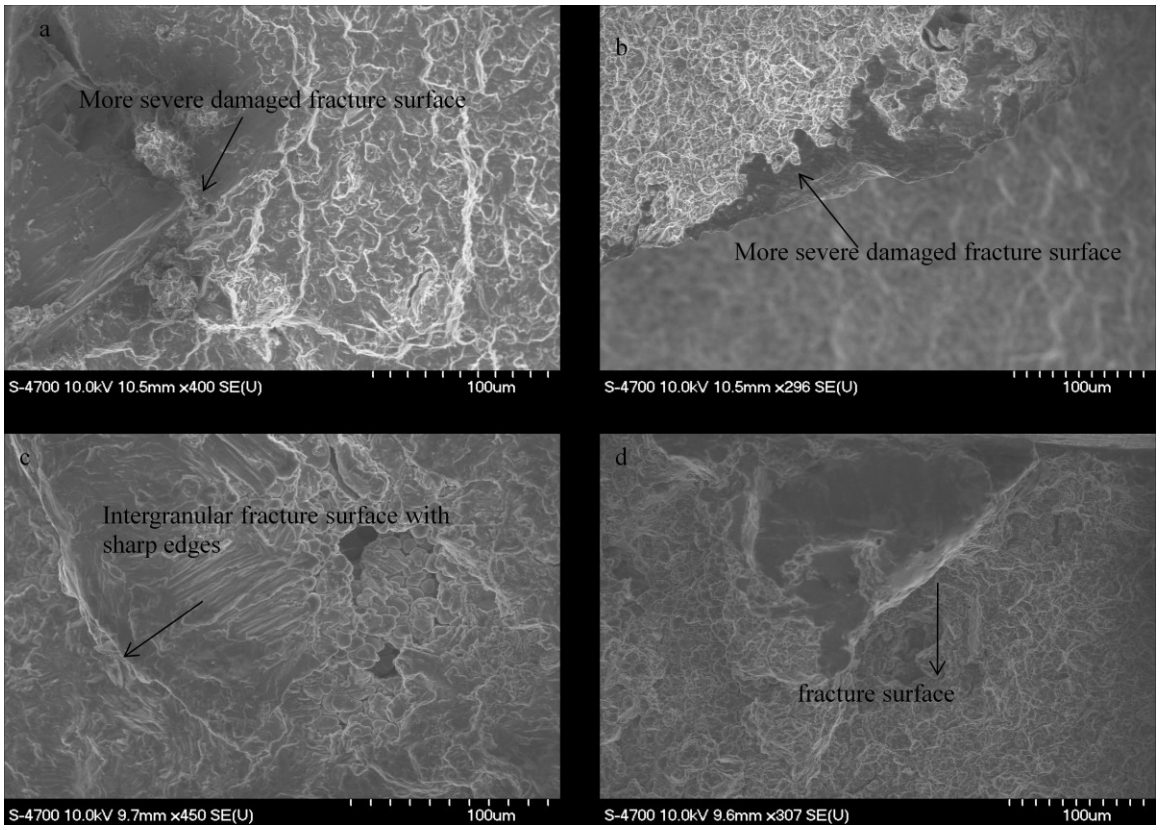

Figure 4.8 Fracture surfaces of the specimens tested at 85 MPa (higher magnification) at room temperature, N_f=64893, (a, b); (c and d) at the cold temperature, N_f=171317.

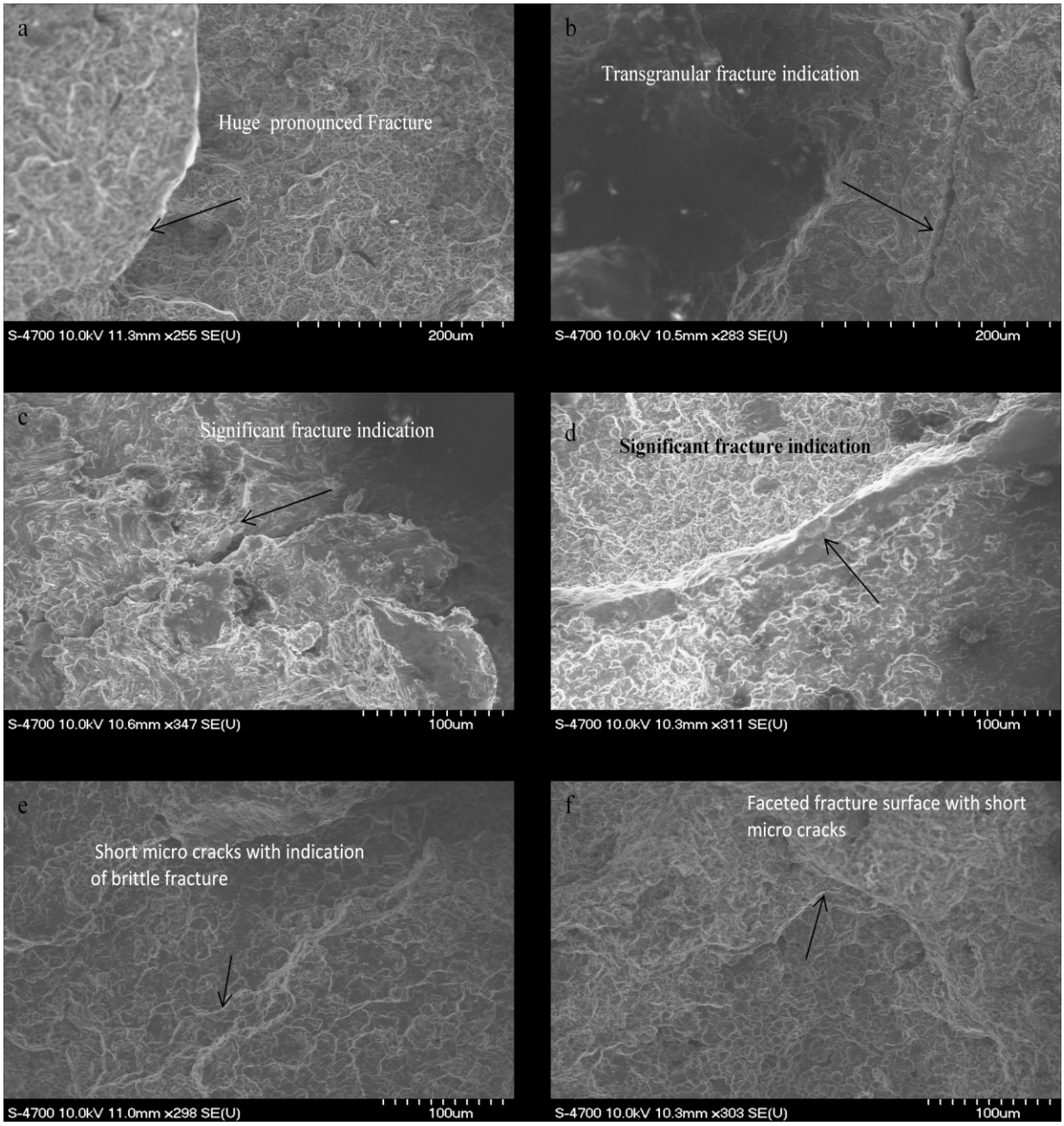

Figure 4.9 Fracture surfaces of the specimens tested at 115 MPa (higher magnification) at room temperature, N_f=38743, (a, b, c, d); (e and f) at the cold temperature, N_f=59658.

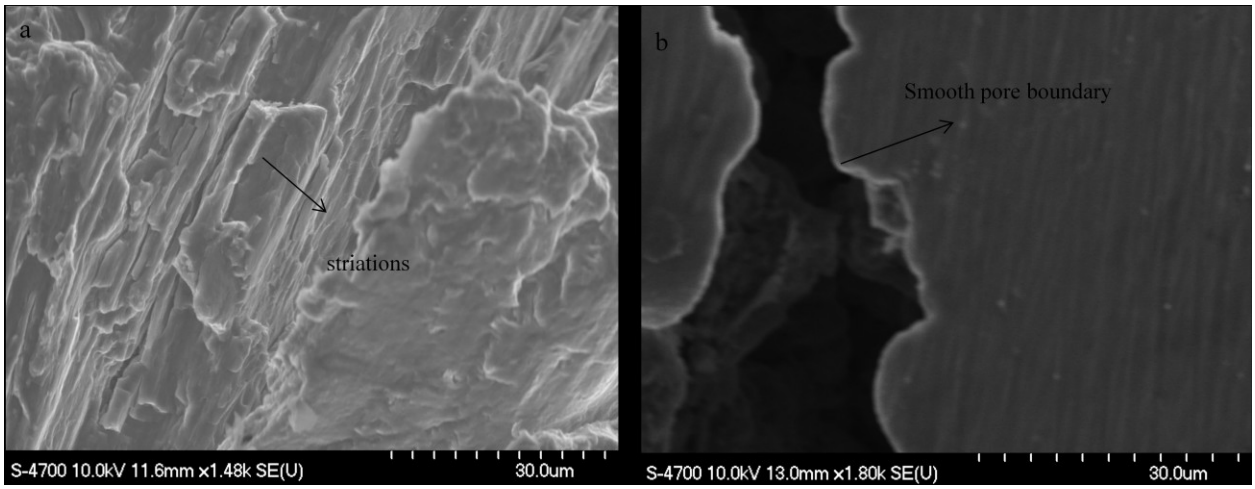

Figure 4.10 (a) SEM images showing large striations found in specimen tested at room temperature, indicating plastic sharpening and blunting; (b) smooth pore boundary region found in the specimen tested at the low temperature.

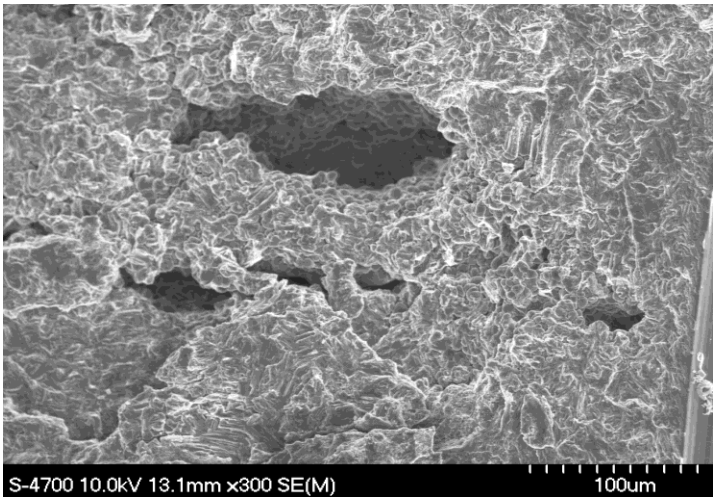

Figure 4.11 Shrinkage porosities found in SEM images.

4.5 CONCLUSION

At low temperature (-40°C), the fatigue life of HPDC AM60B magnesium alloy was observed to increase, as compared to the fatigue life at room temperature. This increase is much more significant at low stress levels than at high stress levels; the difference was found to be almost twice on average.

A difference was also observed in the fracture surfaces of HPDC AM60B magnesium alloy. The reflectivity observed in the SEM images of the fracture surfaces of the specimens tested at room temperature was relatively dull, indicating a relatively ductile fracture. In comparison, shiny and faceted surfaces were observed for the specimens at the low temperature, thereby revealing a brittle fracture mode.

It is believed that at the low temperature, the existence of large stress concentration regions at the grain boundaries of HPDC AM60B magnesium alloy because brittle intergranular fracture with microvoid coalescence, as observed through the SEM images of fracture surfaces of the specimens.

Large variation in the fatigue behavior was also observed, which is believed to be due to the variation in the porosity size and distribution within each specimen.

4.6 ACKNOWLEDGEMENT

This research is carried out with the financial support provided by AUT021 Network of Centers of Excellence, an automotive research and development program focusing on issues relating to the automobile in the 21st century. We are indebted to AUTO 21 for the financial support and IRM (The Institute for Research in Materials, Dalhousie University) for using SEM.

4.7 REFERENCES

ASTM E-8M standard, (2003). Test methods of tension testing of metallic materials [metric]. Annual book of ASTM: Volume 03.01, *American Society of Metals*. Metals Park, Ohio. pp. 83-104.

ASTM E-466 standard, (2003). Standard practice for conducting force controlled constant amplitude axial fatigue tests of metallic materials. *Annual book of ASTM*: Volume 03.01, *American Society of Metals*. Metals Park, Ohio. pp. 515-519.

Gjestland, H., Sannes, S., Wesstengen, H., & Albright, D. (2003). Effect of casting temperature, section thickness and die filling sequence on microstructure and mechanical properties of high pressure die-casting. *NADCA Transactions* , pp. 03-36.

Grinberg, N., Serdyuk, V., Ostapenko, I., Malinkina, T., & Kamyshkov, A. (1979). Effect of low temperature on fatigue failure of magnesium alloy MA12. Khimicheskaya Mekhanika Materialov, pp. 21-25.

Horstemeyer, M., Yang, N., Ken, G., McDowell, D., Fan, J., & Gullett, P. (2004). High cycle fatigue of a die cast AZ91E-T4 magnesium alloy. *Acta Materialia Inc 52*, pp. 1327-36.

Kleiner, S., Beffort, O., Wahlen, A., & Uggowitzer, P. (2002). Microstructure and mechanical properties of squeeze cast and semisolid cast Mg-Al alloys. *Journal of Light Metals 2*, pp. 277-80.

Koch, T.A. (2004). *Fatigue properties of high pressure die cast magnesium AM 60.* M.A.Sc. Thesis, Dalhousie University, Department of Mining and Metallurgical Engineering, Halifax, Nova Scotia, Canada.

Li, W., & Zhang, X. (2001). Investigation of initiation and growth behavior of short fatigue emanating from a single edge notch specimen using in situ SEM. *Material Science and Engineering A Eng 318*, pp. 129-36.

Lu, Y. (2008). *Fatigue properties of high pressure die cast magnesium AM 60B alloy using experimental and computational investigations.* PhD. Thesis, Dalhousie University, Materials Engineering, Halifax, Nova Scotia, Canada.

Lu, Y., Taheri, F., & Gharghouri, M. (2008a). Monotonic and cyclic plasticity responses of high pressure die cast AM60B magnesium alloy. To appear in *Strain*.

Lu, Y., Taheri, F., & Gharghouri, M. (2008b). Study of fatigue crack incubation and propagation mechanisms in a HPDC AM60B magnesium alloy. *Journal of Alloys and Compound 466*, pp. 214-227

Mann, T. (2007). The influence of mean stress on fatigue crack propagation in aluminum alloy. *International Journal of Fatigue 29*, pp. 1393–1401.

Sajuri, Z., Miyashita, Y., & Mutoh, Y. (2005). Effects of humidity and temperature on the fatigue behaviour of an extruded AZ61 magnesium alloy. *Fatigue Fracture of Engineering Material and Structure 28*, pp. 373-379.

Sun, Z., Zhou, M., Hu, H., & Li, N. (2007). Strain-Hardening and fracture behavior of die cast magnesium alloy. *Research Letters in Materials Science*. Volume 2007, Article ID 64195.

Venkateswarana, P., Ganesh Sundara Ramana, S., Pathaka, S., & Miyashitab, Y. (2004). Fatigue crack growth behaviour of a die-cast magnesium alloy AZ91D. *Materials Letters 54*, pp. 2525-2529.

Wang, X., & Fan, J. (2006). An evaluation on the growth rate of small fatigue cracks in cast AM50 magnesium alloy at different temperatures in vacuum conditions. *International Journal of Fatigue 28*, pp. 79-86.

Wang, X., & Fan, J. (2004). SEM online investigation of fatigue crack initiation and propagation in notched cast magnesium specimens. *Journal of Material Science 39(7)*, pp. 2617-20.

Zenner, H., & Renner, F. (2002). Cyclic material behavior of magnesium dies castings and extrusions. *International Journal of Fatigue 24*, pp. 1255-60.

Zhou, M. (2004). *An experimental study of die and squeeze cast Mg alloy AM50.* M.S. thesis. University of Windsor, Department of Mechanical, Automotive & materials Engineering, Windsor, Ontario, Canada.

CHAPTER 5: ANALYSIS OF LEFM PARAMETERS AND FATIGUE PROPAGATION OF SINGLE EDGE NOTCHED TENSION (SENT) CRACKED AM60B MAGNESIUM ALLOY

Md. Nur Hossain and Dr. Farid Taheri

Publication Status: Accepted in COM 2010, 49th Annual Conference, Vancouver, BC. Canada

5.0 ABSTRACT

Analysis of linear elastic fracture mechanics (LEFM) parameters via the Virtual Crack Closure Technique (VCCT) has been obtained for single edge notch tension (SENT) specimens of AM60B magnesium alloy. It is found that the ratio of initial crack length to initial monotonic plastic zone size is one of the critical factors in establishing the limit of using LEFM concepts. If this ratio is below a certain limit (i.e. when crack lengths are small in comparison to the plastic zone size), loss of similitude stress intensity factor range would occur. This ratio, therefore describes the limit below which the use of LEFM would no longer be admissible. In this study, the above limit was established for AM60B magnesium alloy. In addition, fatigue crack propagation tests were conducted to establish the fatigue response of the alloy and determination of the coefficients of the Paris model.

Keywords LEFM (Linear Elastic Fracture Mechanics), VCCT (Vertical Crack Closer Technique), SENT (Single Edge Notch Tension), FCGR (Fatigue Crack Growth Rate), FEM (Finite Element Method)

5.1 INTRODUCTION

Evaluation of the fatigue life of structural components when subject to repeated loading is an important area of engineering. The term 'fatigue' refers to the progressive localized permanent deformation or deterioration of the strength of a structural component due to cyclic or repeated loading. The failure due to cyclic loading may occur at the yield stress level or even below that level. The failure may be defined as the initiation of a crack of visible size or the growth of a visible crack to a critical crack size, leading to catastrophic failure (Dowling, 1998). Under the application of cyclic loading, damage initiates first at the molecular level and then that molecular damage proceeds to become a micro-crack. Due to the stress intensity dislocation, permanent deformations occur in the high stress regions; as a result, a crack would be initiated. The number of cycles used to cause a visible crack is defined as the crack initiation life, N_i. When the micro crack forms, it proceeds to a critical crack size in a stable manner and then extends rapidly leading to a permanent failure. The number of cycles taken for the crack to go from initial size to the critical size is referred to as the crack propagation life, N_P. The sum of the above two lives is referred to as the total life, N. Depending on the material, for some structural components, the majority of the total life may be consumed for initiating a crack and less for propagation; whereas in other materials, the propagation life may take the majority of the total life, and less for initiation. By using the principles of fracture mechanics, crack propagation life can be calculated. Although it is not possible yet to understand clearly the complete fundamental mechanism of fatigue failures, some useful engineering models are available and these can be used to predict the crack initiation and propagation lives.

Materials, especially those with relatively low fracture toughness, might fail even below their ultimate strength. The failure can be analyzed on the basis of elastic concepts, through the use of the linear elastic fracture mechanics (LEFM) (Stephens et al., 1980). High strength light weight metallic alloys, such as those used in aerospace industry, are examples of such materials (Stephens et al., 1980). Although LEFM is applicable for such materials, there are some limitations for the use of LEFM, in terms of crack length, stress level, plastic zone size and other parameters. A means to establish whether LEFM

would be admissible is by evaluating the ratio between the initial monotonic crack length and plastic zone size, which is the focus of this study.

Using LEFM analyses (i.e., the stress intensity factor range, ΔK), it is possible to make a direct comparison of fatigue crack growth behavior between actual engineering components or structures and laboratory specimens. In this study experimental tests were conducted to determine the fatigue crack growth rate of AM60B magnesium alloy. LEFM analyses were conducted for different crack lengths. In addition, two crack propagation models were used for determining the fatigue crack growth rate (FCGR) of AM60B magnesium alloy, using the NISA/ENDURE finite element code (Nisa/Endure, 1992). The virtual crack closure technique (VCCT) was used in the fracture mechanics analysis part.

5.2 THEORETICAL BACKGROUND

5.2.1 Linear Elastic Fracture Mechanics Approach

In the VCCT, as shown schematically in Figure 5.1, the strain energy release rate is computed through calculation of the nodal forces and displacements (Anderson, 2000). From a finite element perspective, both regular low order singular and collapsed elements can be used for calculating VCCT, leading to accurate results; VCCT is therefore widely used in progressive failure analysis. Moreover, VCCT is not very sensitive to the finite element mesh size. As a result, even with using coarse meshes for modeling the crack tip, accurate results can be obtained. Due to this reason, VCCT is easy to apply, eliminating the extra effort required for mesh refinement demanded by the other relevant techniques. Nowadays, VCCT is implemented into several finite element software packages, like the GENOA/PFA, ABAQUS, NISA/ENDURE and other progressive failure analysis tools (Anderson, 2000).

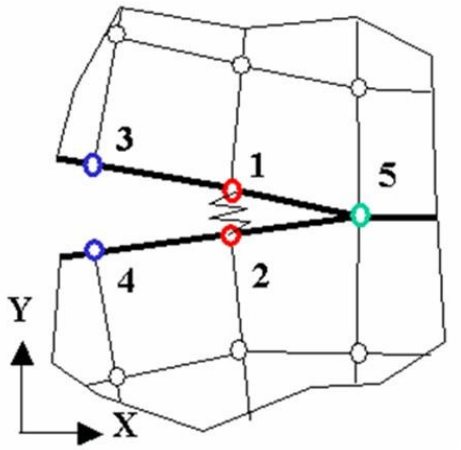

Figure 5.1 Schematic of the virtual crack closure technique (Anderson, 2000).

The formulation for evaluating the strain energy release rate used by VCCT is given below (Anderson, 2000):

$$G_I = \frac{F_{Y_{12}} v_{34}}{2t\Delta a} \tag{5-1}$$

$$G_{II} = \frac{F_{X_{12}} u_{34}}{2t\Delta a} \tag{5-2}$$

Where, G_I and G_{II} are the Strain energy release rate components for Mode I (the opening mode) and Mode II (the sliding mode), respectively. The two quantities $F_{X_{12}}$ and $F_{Y_{12}}$ are the nodal forces between nodes 1 and 2 along the X and *Y* directions, and, u_{34} and v_{34} are the separation displacements between nodes 3 and 4 along *X* and *Y* direction, respectively, while Δa is the virtual crack extension and *t* is the plate thickness.

5.2.2 Fatigue Crack Growth Rate Based on Paris Model

LEFM was originally developed to describe fracture behavior in materials, and later it was extended for assessment of fatigue crack growth under mainly elastic conditions. However, it has been shown that LEFM concepts can be used in situations where limited plasticity exists, so long as the plasticity is confined to the crack tip region.

Crack growth data can be obtained by subjecting a laboratory specimen to cyclic loading. The specimen may be of various configurations, as long as the geometric factor is known, so that the stress intensity factors can be evaluated. When testing a specimen, the crack length, *a*, is monitored at regular intervals and the corresponding numbers of cycles are recorded at each crack growth interval. By plotting the crack growth increment versus the associated cycles, the rate of growth *(da/dN)* can be obtained. From the plot of *da/dN* versus the stress intensity factor range, the required parameters for fatigue crack propagation (FCP) models were estimated. For example, the Paris model is presented by the following equation (Anderson, 2000).

$$\frac{da}{dN} = C_P(\Delta K)^{m_p} \tag{5-3}$$

where ΔK is the range of stress intensity factor (SIF), C_p and m_p are constants obtained by fitting a straight line through the data in the second linear segment of *da/dN* versus ΔK curve [(Dowling,1998), (Stephens et al., 1980) and (Broek, 2001)].

5.3 MATERIAL AND EXPERIMENTAL METHODS

Test specimens were extracted from die cast AM60B Mg alloy plates provided by Meridian Technologies Inc., (Strathroy, Ontario). The chemical composition of the alloy is shown in Table 5.1 [(Lu, 2008), (Koch, 2004), and (Lu et al. 2008a)].

Table 5.1 Composition of cast AM60 magnesium alloy in weight %

Alloy	Al	Mn	Si	Zn	Cu	Fe	Ni	Other	Mg
Cast AM60B	5.5-6.5	0.25 Min	0.10 Max	0.22 Max	0.010 Max	0.005 Max	0.002 Max	0.003 (Total)	Bal.

The single edge notch tension (SENT) specimens were used for fatigue crack growth tests. The specimens were prepared according to ASTM E647 standard (ASTM E-647, 1996).

The mechanical properties of the alloy were measured by uniaxial tensile tests, conforming to ASTM E8 (ASTM E-8M, 2003). The yield stress, σ_y, was determined to be 150 MPa; the ultimate tensile strength was evaluated to be 240 MPa.

The fatigue crack propagation cyclic testing was conducted using a servo-hydraulic Instron 8501 machine with the Test Star control system. The tests were performed under load control, at a stress ratio R=0.1, with the maximum stress of 80 MPa and frequency of 30 Hz. The incremental lengths of fatigue cracks were measured directly with a calibrated digital vernier attached to a microscope unit as shown in Figure 5.2.

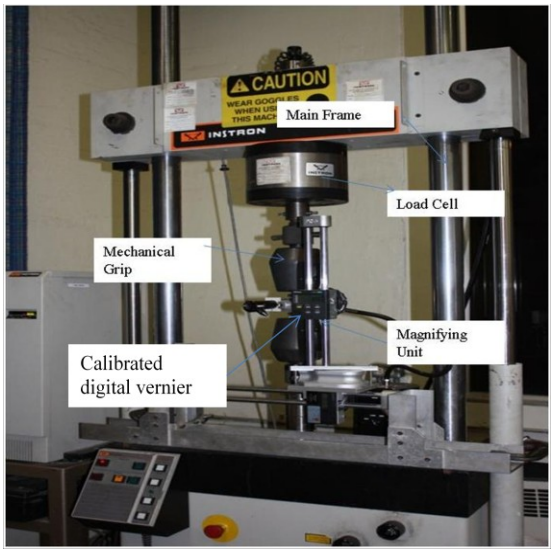

Figure 5.2 Experimental setup of fatigue crack propagation tests.

The specimens were first notched by a jeweler's saw, and subsequently fatigue cracked to introduce a sharp crack for the actual fatigue crack growth test. Once the fatigue precrack was formed, extension of the growing crack was recorded in terms of crack length increment and the associated number of cycles. The recording was continued until the specimen had failed. The *'a'* versus N_f curves were plotted for each specimen, as illustrated in Figure 5.5. The data was subsequently post-processed to generate *da/dN* versus ΔK data.

5.4 RESULTS AND DISCUSSION

5.4.1 Limit Plastic Zone Size and Applied Stress for LEFM Analysis

To determine the stress intensity factor for various crack lengths and stresses, LEFM was used via VCCT, as explained earlier. Finite element modeling was conducted using the NISA code. NISA's plane stress element (NKTP 1) was used to construct the model (Nisa/Endure, 1992). Due to symmetry in geometry and boundary conditions, only half of the specimen had to be modeled. The crack tip singularity was simulated by the "quarter-point" technique. The main objective was to evaluate the stress intensity factor for the SENT specimen for different crack lengths, at various stress levels so that the limit plastic zone size could be established and compared to the values established analytically, using the following fundamental equation [(Stephens et al. 1980) and (Broek, 2001)]:

$$K = Y\sigma\sqrt{\pi a} \tag{5-4}$$

In the above equation, Y is a geometric factor which is taken as 1.12 for SENT specimens, as recommended by ASTM E647, σ is the nominal tensile stress and a, is the crack length.

Figure 5.3 compares the analytical results of stress intensity factor at stress levels 40, 80 and 120 MPa for various crack lengths, (i.e. 1 to 6 mm), with the computational results produced by finite element. Although there are some differences among the analytical results, and those obtained by the finite element method in the region of lower crack lengths, nevertheless a reasonable overall agreement is obtained. For example, at stress values 80 and 120 MPa, there are some differences for crack lengths up to 3 mm. And at 40 MPa stress value there is some difference for initial crack length.

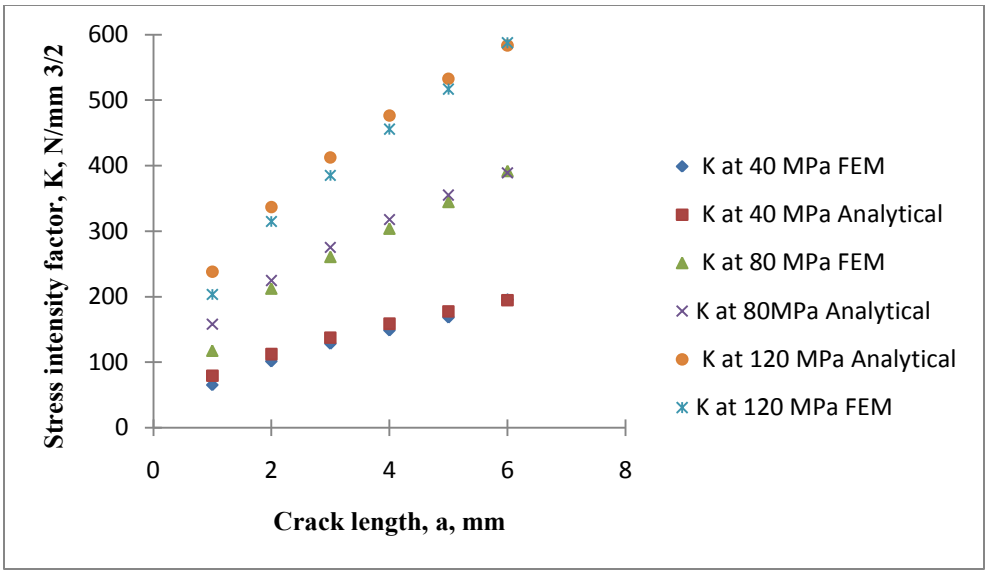

Figure 5.3 Comparison of the theoretical and computational stress intensity factors vs. crack length at different stress level.

5.4.1.1 Establishment of the Limiting Factors for Applicability Of LEFM For AM60B Magnesium Alloy

The plastic zone size and stress level are two vital parameters for establishing the limit of applicability of LEFM for use with the AM60B magnesium alloy. To establish the above limiting parameters, theoretical calculations, verified by FEM were carried out for various stress levels. The initial monotonic plastic zone size was calculated first. For this, the initial value of K_{max} was calculated using equation 5-4. For example for σ_{max}= 120 MPa and a_i=1 mm, K was determined to be 238 N/mm$^{3/2}$

Since, the tested plates were thin, plane stress would prevail and equation 5-5 can be used to calculate the radius of the plastic zone [(Stephens et al., 1980) and (Broek, 2001)].

$$r_y = \frac{1}{2\pi}\left(\frac{K}{\sigma_y}\right)^2 \tag{5-5}$$

In the above equation, r_y is plastic zone size, σ_y is the yield stress and K is the stress intensity factor.

Figure 5.4 presents the monotonic plastic zone size for AM60B magnesium alloy at various initial crack lengths and stress levels.

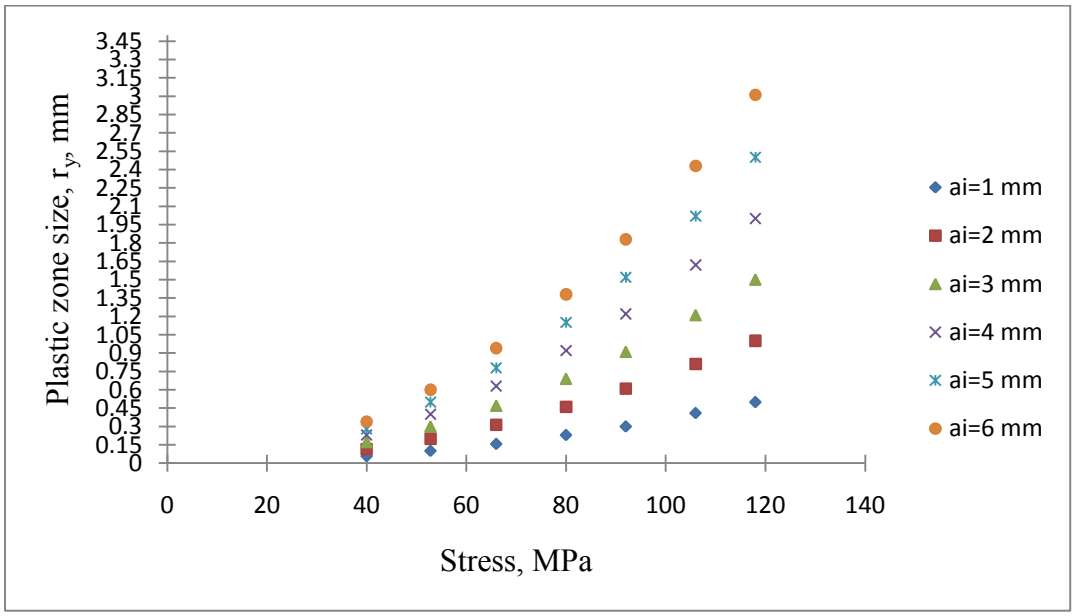

Figure 5.4 Variation of plastic zone size calculated for different stress levels and initial crack lengths.

The ratio of the initial crack length to plastic zone size was established as 17.54, 10.00, 6.36, and 3.33, corresponding to nominal stress values of 40, 52.6, 66, and 70 MPa, respectively, for the initial crack length of 1 mm. From the above results, it is clear that at stress level greater than 52.6 MPa, the ratio does not fall within the general restriction of $a/r_y \geq 8$ (Broek, 2001). Therefore, limiting marginal value of stress below which LEFM is applicable would be within 52.5-66 MPa, for initial crack length of 1 mm, according to the above configuration. In the same way, one can determine the limiting values of stress values and the ratio of the initial crack length to plastic zone size for other configurations. The comparison of the values established analytically and those by finite element are shown in Table 5.2. In the Table 5.2 the theoretical (THR) value of stress intensity factor is based on equation 5-5.

Table 5.2 : Comparison of the analytical and FEM results for plastic zone size at three stress levels.

Stress Value (MPa)	r_y at a_i=1.00 mm		r_y at a_i=2.00 mm		r_y at a_i=3.00 mm		r_y at a_i=4.00 mm		r_y at a_i=5.00 mm		r_y at a_i=6.00 mm	
	FEM	THR	FEM	THR	FEM	THR	FEM	THR	FEM	THR	FEM	THR
40	0.04	0.05	0.10	0.15	0.15	0.20	0.20	0.25	0.26	0.25	0.35	0.30
80	0.13	0.25	0.41	0.50	0.62	0.75	0.84	1.00	1.08	1.15	1.40	1.50
120	0.38	0.50	0.90	1.00	1.35	1.50	1.90	2.00	2.43	2.50	3.15	3.00

Note: FEM refers to finite element method's results and THE refers to the theoretical results obtained by using Equation 5-5

5.4.2 Fatigue Crack Growth Rate Based On the Paris Model

In many studies, it has been shown that fatigue crack growth rate can be evaluated as a function of the equivalent stress intensity factor range, evaluated at room or higher temperatures, using the Paris model (i.e. equation (5-3)) [(Dowling, 1998) (Stephens et al., 1980) (Broek, 2001)]. The Paris model has also been extended to determine fatigue crack growth rate (FCGR) by accounting for the stress ratio; *R.* Walker [(Stephens et al., 1980), (Broek, 2001), and (Wang & Fan, 2006)], proposed that crack propagation rate can be related to the equivalent range of SIF, ΔK_{eq}, using the following relationship:

$$\frac{da}{dN} = C_P(\Delta K_{eq})^{m_p} \tag{5-6}$$

Where:

$$\Delta K_{eq} = \Delta K/(1-R)^{1-\gamma} \tag{5-7}$$

and: $$\Delta K = Y\Delta\sigma\sqrt{\pi a_{avg}} \tag{5-8}$$

In the above equation C_P is the Paris constant, $\frac{da}{dN}$ is the fatigue crack growth rate, ΔK indicates the stress intensity factor range, m_p is the Paris exponent, Y is the geometric factor and γ is a material parameter ranging from 0.3 to 0.8 [(Dowling,1998), (Broek, 2001), and (Anderson, 1980)].

Figure 5.5 shows, the variation of crack length versus the number of applied cycles for three identical SENT test specimens of AM60B magnesium alloy, subjected to cyclic load with a maximum stress amplitude of 80 MPa and R=0.1. All specimens contained the same initial crack length a_i=1 mm. From the figure, it is clear that growth rate is increased with increasing cycle for the specimens tested. The reason for the variation in the behavior is postulated to be due to variation in the porosity size and distribution within each specimen.

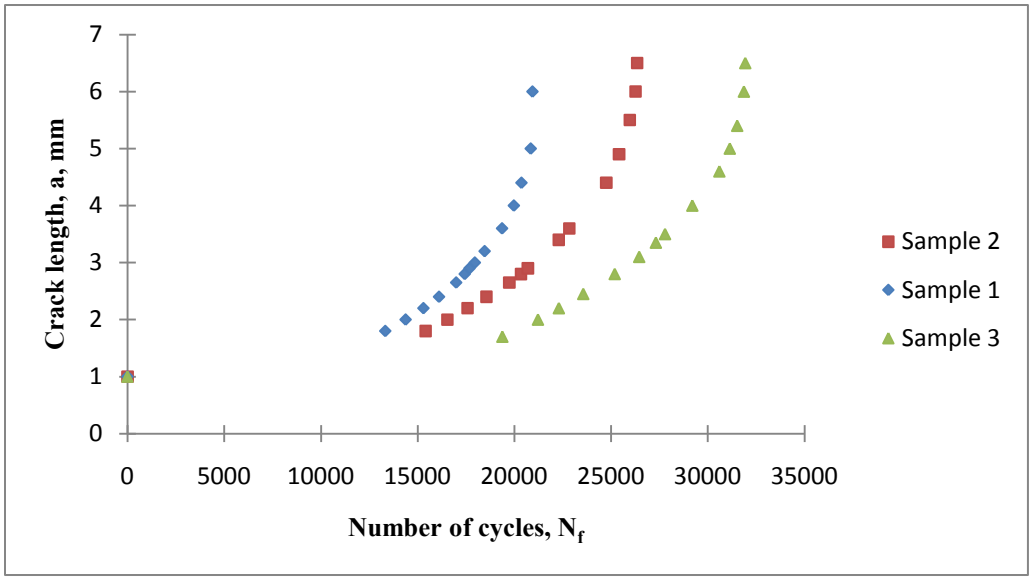

Figure 5.5 Fatigue Crack growth propagation for the SET specimens of AM60B magnesium alloy.

It is well established that for a given initial crack size, the fatigue life depends on the magnitude of the applied stress and the fracture resistance of the material [(Stephens et al., 1980) and (Broek, 2001)]. With applying LEFM, the data is converted to the format shown in Figure 5.6, which is suitable for FCGR assessment. The procedure entails the

evaluation of the stress intensity factor range, ΔK, for a given crack growth rate da/dN. As seen in Figure 5.6, higher crack growth rate is observed for specimen 1 and the rate is lower for specimens 2 and 3.

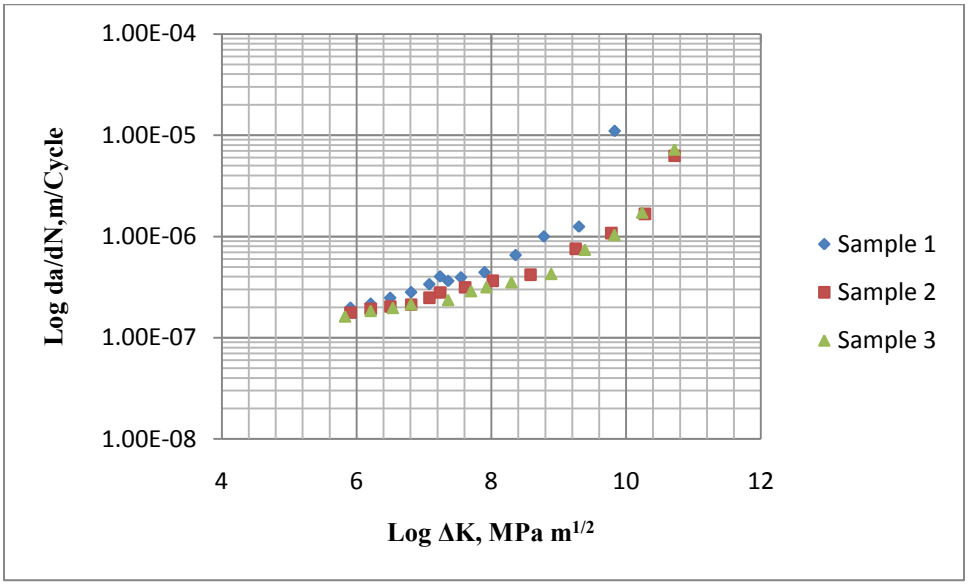

Figure 5.6 Plot of da/dN vs. ΔK for the three tested specimens.

As stated earlier, at positive stress ratios, the exponent γ usually takes values between 0.3 and 0.8, where γ=0.3 gives a strong dependence on R while γ=0.8 denotes a weaker dependence on R (Stephens et al., 1980).The Walker relationship allows approximations of the material constants for various stress ratios; therefore, we use the Walker relationship in the present work. The exact value of γ is not known for AM60B magnesium alloy at stress ratio of R=0.1. So, it is assumed that γ=0.5, which is known to produce a reasonable estimate [(Wang & Fan, 2006) and (Mann, 2007)].

Figure 5.7 illustrates the variation of growth rate with respect to stress intensity factor range, according to the Walker and Paris models for the SENT specimens. Due to the stress ratio consideration, the growth rate is greater using the Walker model in comparison to that obtained based on the Paris model. As seen, the variation of the growth rate is more pronounced at high stress intensity factor ranges for all three specimens, as well as the growth rate being higher for specimen 1 than 2 and 3.

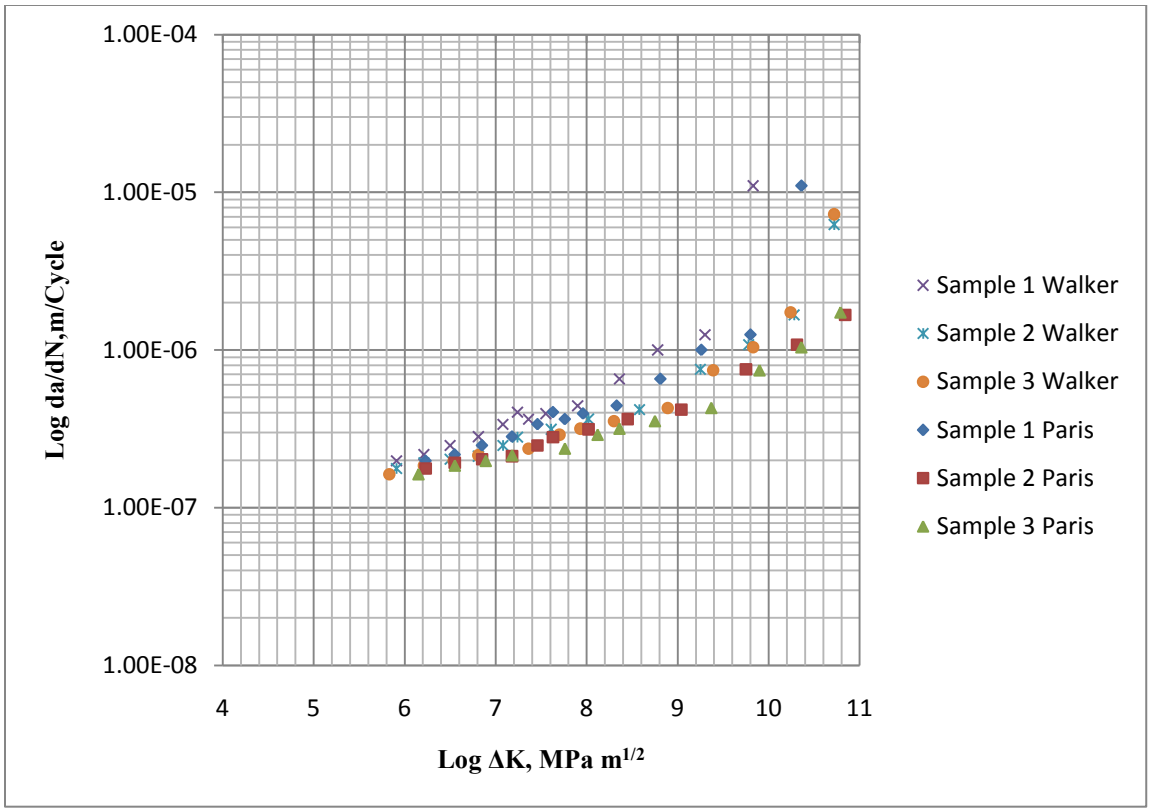

Figure 5.7 Plot of *da/dN* vs. *ΔK* for both the Paris and Walker models.

From the linear portion of the above curves, the Paris exponent, m_p, was found to be 3.91 (the average value) with Paris constant $7x10^{-11}$ (also the average value), which was used in FEM to determine the growth rate for the comparison with the analytical results.

5.5 CONCLUSION

The procedure outlined in this study, and the comparison of the computational results and those obtained experimentally revealed that LEFM is admissible for assessing the fatigue characteristics of the AM60B magnesium alloy. However, there exists a limit of applicability, which depends on the value of the applied stress and the ratio of the initial crack length to monotonic plastic zone size.

These limiting parameters were evaluated for the alloy by LEFM approach for SENT cracked specimens of AM60B magnesium alloy, having initial crack lengths ranging from 1 mm to 6 mm, the limiting stress value which was established is not above 52.6

MPa, to provide the limit of the ratio, $a_0/r \leq 8$ (i.e. the ratio between initial crack lengths to plastic zone size).

Walker's equation can be used to account for the effect of stress ratio when estimating the crack growth rate. Subsequently, Paris constant C and exponent m, were evaluated as $7x10^{-11}$ and 3.91 (based on average value of three specimens), respectively. These values can be used to characterize the fatigue crack propagation and life expectancy of AM60B under various stress ratios.

Fatigue growth rates calculated from the experimental results and fall within $3.5x10^{-6}$ mm/Cycle to $3.06x10^{-8}$ mm/Cycle (for all tests), which shows a good comparison with the growth rates found based on the FEM results. The variation of growth rate is more pronounced at high stress intensity factor range in all three specimens.

5.6 ACKNOWLEDGEMENT

This research is carried out with the financial support provided by AUT021 Network Center of Excellence, an automotive research and development program focusing on issues relating to the automobile in the 21st century. We are indebted to AUTO 21 for the financial support and IRM (The Institute for Research in Materials, Dalhousie University) for using SEM.

5.6 REFERENCES

Anderson, T.L. (2000). Fracture Mechanics: fundamentals and applications, second edition. *CRC Press, Inc*. FL, USA. pp. 573-577.

ASTM E-8M standard, (2003). Test methods of tension testing of metallic materials [metric]. Annual book of ASTM: Volume 03.01, *American Society of Metals*. Metals Park, Ohio. pp. 83-104.

ASTM E-466 standard, (2003). Standard Practice for Conducting Force Controlled Constant Amplitude Axial Fatigue Tests of Metallic Materials. Annual book of ASTM: volume 03.01, *American Society of Metals*. Metals Park, Ohio. pp. 515-519.

Broek, D. (2001). The Practical Use of Fracture Mechanics. *FractuREsearch Inc*. Galena, OH, USA. pp. 44-86.

Dowling, N. (1998). Mechanical Behavior of Materials. *Prentice-Hall: Inc*. New Jersey, USA.

Koch, T.A. (2004). Fatigue properties of high pressure die cast magnesium AM 60. M.A.Sc. Thesis, Dalhousie University, Department of Metturgical Engineering. Halifax, Nova Scotia, Canada.

Lu, Y. (2008). Fatigue properties of high pressure die cast magnesium AM 60B alloy using experimental and computational investigations. PhD. Thesis, Dalhousie University, Materials Engineering. Halifax, Nova Scotia, Canada.

Lu, Y., Taheri, F., & Gharghouri, M. (2008a). Monotonic and cyclic plasticity responses of high pressure die cast AM60B magnesium alloy. To appear in *Strain*.

Lu, Y., Taheri, F., & Gharghouri, M. (2008b). Study of fatigue crack incubation and propagation mechanisms in a HPDC AM60B magnesium alloy. *Journal of Alloys and Compound* 466, pp. 214-227.

Mann, T. (2007). The influence of mean stress on fatigue crack propagation in aluminum alloy. *International Journal of Fatigue 29*, pp. 1393–1401.

Stephens, R., Fatemi, A., Stephens, R., & Fuchs, H. (1980). *Metal Fatigue in Engineering.* John Wiley & Sons, Inc., New Jersey, NJ, USA.

Wang, X., & Fan, J. (2006). An evaluation on the growth rate of small fatigue cracks in cast AM50 magnesium alloy at different temperatures in vacuum conditions. *International Journal of Fatigue 28*, pp.79-86.

CHAPTER 6: CONCLUSIONS

6.0 CONCLUSIONS

The following findings are summarized according to the outcome of the research project.

- At an elevated temperature of 80°C, the fatigue life of AM60B magnesium alloy was decreased as compared to room temperature. On the other hand, at a low temperature of -40°C the number of cycles to failure was increased. For the condition of elevated temperature, and at low stresses, the decrease was not as pronounced as that observed at high stresses. However, at the low temperature condition, at low stresses, the increase was much more significant than that observed at higher stresses.
- The comparison of the analytically calculated results with those obtained from the experiments indicated that the Walker model could be effectively used for predicting the crack growth rate of HPDC AM60B magnesium alloy at various stress ratios. For R=0.1, the initial growth rate was found to be $2x10^{-7}$ m/cycle, whereas for stress ratio R=0.2, the initial growth was increased to $6x10^{-7}$ m/cycle. These results can be extrapolated in order to establish the fatigue crack growth response of AM60B magnesium alloys under different loading ratios. The finite element results were found to be very close to the experimental results. Further experimental studies are however needed to confirm that the above would also hold for other stress ratios and temperatures.
- At the elevated temperature, the fatigue-generated micro-cracks mainly cleaved the α-Mg grains. The micro-cracks propagated preferentially through the dendrite cells and along the interdendritic region. Large segregation of brittle eutectic β-$Mg_{17}Al_{12}$ along the grain boundaries cleaved the α-Mg grains at elevated temperature. Moreover, at the higher temperature, the fatigue micro-cracks further propagated, passing through to the α-Mg grains, because these regions had softened due to the elevated temperature. On the other hand, the commencement of fatigue micro-cracks occurred in cast magnesium AM60B alloys generally occurred along the interfaces of the α-Mg and β-$Mg_{17}Al_{12}$ grains. This occurred due to the micro-mechanism of the accumulative plastic slipping of surface grains (α-Mg) and deformation mismatch of two phases. A dull ductile fracture was observed in the SEM images of fracture surfaces of the samples tested at room

temperature, whereas shiny and faceted surfaces signified brittle fracture for the samples tested at low temperatures.

- The initiation point of cracks began due to the existence of internal discontinuity caused by the presence of porosity. The final fracture resulted from the growth and coalescence of the cracks, as was confirmed by the SEM images of fatigue crack propagation. The reason for the variation in the behavior is believed to be due to variation in the porosity size and distribution within each specimen.
- There exists a limit for admissibility of the application of LEFM when investigating the fatigue response of the alloy; this limit depends on the value of the applied stress and the ratio of the initial crack length compared to the monotonic plastic zone size. These limiting parameters were evaluated for the alloy by the LEFM approach for SENT cracked specimens of AM60B magnesium alloy, having initial crack lengths ranging from 1 mm to 6 mm. The limiting stress value which was established did not exceed 52.6 MPa, producing the limiting ratio of $a_0/r \leq 8$ (i.e. the ratio between initial crack lengths to plastic zone size).
- By using Walker's equation, it is possible to account the effect of stress ratio in estimating the crack growth rate. Subsequently, Paris' model constant C and exponent m were evaluated as $7x10^{-11}$ and 3.91 (based on average value of three specimens), respectively. These values, in conjunction with Walker's model, can be used to characterize the fatigue crack propagation and life expectancy of AM60B under various stress ratios.

6.1 RECOMMENDATIONS FOR FUTURE WORK

- In this research, the fatigue and fracture response of AM60B magnesium alloy were characterized based on constant amplitude loading. As most of the structural applications often undergo variable amplitude load patterns, the first recommendation is to conduct the same investigation for conditions of variable amplitude loading. Additionally, supplementary research can be extended to other specimen configuration and loading situations.

- As thermal loads are not constant in most real life applications, the fluctuation of thermal loading may pose a significant consequence on the fatigue response of the alloy. This issue should be considered in the future works.

- Another recommendation is to investigate the influence of other modifying factors on fatigue and fracture characterization of HPDC AM60B magnesium alloys. For example, size and specimen configuration, notch size, humidity and corrosion could strongly alter the resulting crack propagation rate and fatigue life cycle.

- Variations in the behavior of the alloy were found to be strongly affected by the variation of size and distribution of porosities within each specimen. Thus, it could be worthwhile to control the variation of porosities within specimens to determine the accuracy of the results.

REFERENCES

Anderson, T.L. (2000). Fracture Mechanics: fundamentals and applications, second edition. *CRC Press, Inc*. FL, USA. pp. 573-577.

ASTM E-8M standard, (2003). Test methods of tension testing of metallic materials [metric]. Annual book of ASTM: Volume 03.01, *American Society of Metals*. Metals Park, Ohio. pp. 83-104.

ASTM E-466 standard, (2003). Standard practice for conducting force controlled constant amplitude axial fatigue tests of metallic materials. Annual book of ASTM: Volume 03.01, American Society of Metals. Metals Park, Ohio. pp. 515-519.

ASTM E-647 standard, (1996). Standard practice for conducting force controlled constant amplitude axial fatigue tests of metallic materials. Annual book of ASTM: volume 03.01. Metals Park, Ohio.

Broek, D. (2001). The Practical Use of Fracture Mechanics. FractuREsearch Inc. Galena, OH, USA. pp. 44-86.

Cahn, R., Haasen, P., & Kramer, E. (1996). Structure and Properties of Nonferrous Alloys. *Materials Science and Technology*.

Dowling, N. (1998). *Mechanical Behavior of Materials*. Prentice-Hall Inc. New Jersey, USA.

Dieter, G.E. (1988). Mechanical metallurgy, SI metric edition. McGraw-Hill. ISBN 0-07-100406-8. New York, USA.

Eliezer, A., Gutman, E., Abramov, E., & Unigovski, Y. (2001). Corrosion fatigue of die-cast and extruded magnesium alloys. *Journal of Light Metals 1*, pp. 179-186.

Gjestland, H., Sannes, S., Westengen, H., & Albright, D. (2003). Effect of casting temperature, section thickness and die filling sequence on microstructure and mechanical properties of high pressure die-casting. *NADCA Transactions* , pp. 03-36.

Grinberg, N., Serdyuk, V., & Ostapenko, I. (1977). Features of fatigue failure in magnesium alloy MA12 in air and in vacuum. *Mechanics of Materials 6*, pp. 61-66.

Grinberg, N., Serdyuk, V., Ostapenko, I., Malinkina, T., & Kamyshkov, A. (1979). Effect of low temperature on fatigue failure of magnesium alloy MA12. Khimicheskaya Mekhanika Materialov, pp. 21-25.

Horstemeyer, M., Yang, N., Ken, G., McDowell, D., Fan, J., & Gullett, P. (2004). High cycle fatigue of a die cast AZ91E-T4 magnesium alloy. *Acta Materialia Inc 52*, pp. 1327-36.

Ishihara, S., McEvily, A., Sato, M., Taniguchi, K., & Goshima, T. (2009). The effect of load ratio on fatigue life and crack propagation behavior of an extruded magnesium alloy. *International Journal of Fatigue 31*, pp. 1788-1794.

Kleiner, S., Beffort, O., Wahlen, A., & Uggowitzer, P. (2002). Microstructure and mechanical properties of squeeze cast and semisolid cast Mg-Al alloys. *Journal of Light Metals 2*, pp. 277-80.

Koch, T.A. (2004). *Fatigue properties of high pressure die cast magnesium AM 60.* M.A.Sc. Thesis, Dalhousie University, Department of Mining and Metallurgical Engineering, Halifax, Nova Scotia, Canada.

Laird, C. (1967). The influence of metallurgical structure on the mechanisms of fatigue crack propagation. *The American Society for Testing and Materials* 415, pp. 131-168.

Li, W., & Zhang, X. (2001). Investigation of initiation and growth behavior of short fatigue emanating from a single edge notch specimen using in situ SEM. *Material Science and Engineering A Eng 318*, pp. 129-36.

Lu, Y. (2008). *Fatigue properties of high pressure die cast magnesium AM 60B alloy using experimental and computational investigations.* PhD. Thesis, Dalhousie University, Materials Engineering, Halifax, Nova Scotia, Canada.

Lu, Y., Taheri, F., & Gharghouri, M. (2008a). Monotonic and cyclic plasticity responses of high pressure die cast AM60B magnesium alloy. To appear in *Strain*.

Lu, Y., Taheri, F., & Gharghouri, M. (2008b). Study of fatigue crack incubation and propagation mechanisms in a HPDC AM60B magnesium alloy. *Journal of Alloys and Compound 466*, pp. 214-227

Mann, T. (2007). The influence of mean stress on fatigue crack propagation in aluminum alloy. *International Journal of Fatigue 29*, pp. 1393–1401.

Nisa/Endure Version 92 (1992): *Display III user's manual,* Engineering mechanics Research Corporation., MICHIGAN, USA.

Sajuri, Z., Miyashita, Y., & Mutoh, Y. (2005). Effects of humidity and temperature on the fatigue behaviour of an extruded AZ61 magnesium alloy. *Fatigue Fracture of Engineering Material and Structure 28*, pp. 373-379.

Shih, T., Liu, W., & Chen, Y. (2002). Fatigue of as-extruded AZ61A magnesium alloy, *Materials Science and Engineering A 28* (1-2), pp. 152-162.

Stephens, R., Fatemi, A., Stephens, R., & Fuchs, H. (1980). *Metal Fatigue in Engineering.* John Wiley & Sons, Inc., New Jersey, NJ, USA.

Sun, Z., Zhou, M., Hu, H., & Li, N. (2007). Strain-Hardening and fracture behavior of die cast magnesium alloy. *Research Letters in Materials Science*. Volume 2007, Article ID 64195.

Suresh, S. (1998). *Fatigue of materials* (Second ed.). Cambridge University Press. Cambridge, UK.

Verreman, Y., & Limodin, N. (2008). Fatigue notch factor and short crack propagation. Engineering Fracture Mechanics 75 (6), pp. 1320-1335

Venkateswarana, P., Ganesh Sundara Ramana, S., Pathaka, S., & Miyashitab, Y. (2004). Fatigue crack growth behaviour of a die-cast magnesium alloy AZ91D. *Materials Letters 54*, pp. 2525-2529.

Wang, X., & Fan, J. (2006). An evaluation on the growth rate of small fatigue cracks in cast AM50 magnesium alloy at different temperatures in vacuum conditions. *International Journal of Fatigue 28*, pp. 79-86.

Wang, X., & Fan, J. (2004). SEM online investigation of fatigue crack initiation and propagation in notched cast magnesium specimens. *Journal of Material Science 39(7)*, pp. 2617-20.

Wang, X., & Fan, J. (2006). An evaluation on the growth rate of small fatigue cracks in cast AM50 magnesium alloy at different temperatures in vacuum conditions. *International Journal of Fatigue 28*, pp. 79-86.

Zenga, R., Xub, Y., & Hanb, E. (2009). Fatigue crack propagation behavior of an as-extruded magnesium alloy AZ80. *Materials Science and Engineering A 509*, pp. 1-7.

Zenner, H., & Renner, F. (2002). Cyclic material behavior of magnesium dies castings and extrusions. *International Journal of Fatigue 24*, pp. 1255-60.

Zhou, M. (2004). *An experimental study of die and squeeze cast Mg alloy AM50.* M.S. thesis. University of Windsor, Department of Mechanical, Automotive & materials Engineering, Windsor, Ontario, Canada.